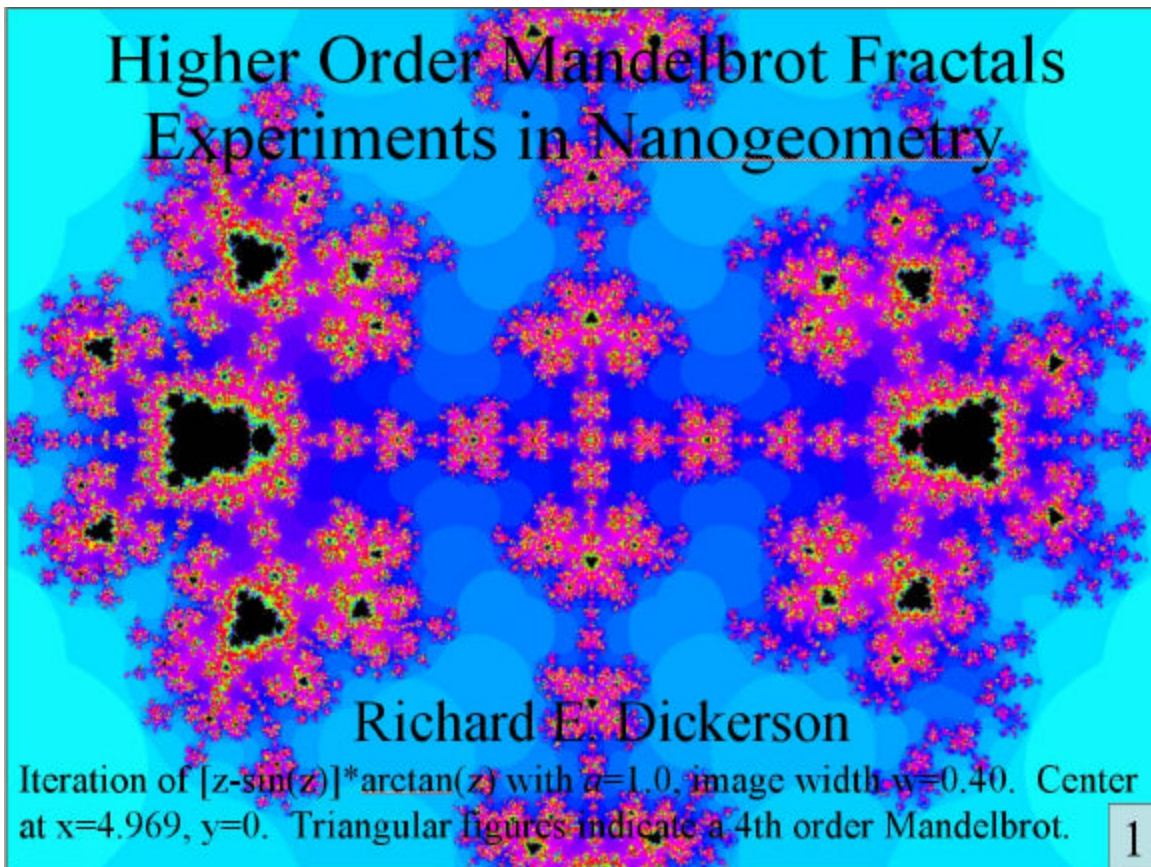


HIGHER ORDER MANDELBROT FRACTALS: EXPERIMENTS IN NANOGOMETRY

Richard E. Dickerson
Molecular Biology Institute, Boyer Hall
University of California, Los Angeles
Los Angeles CA 90095-1570
red@mbi.ucla.edu



CONTENTS

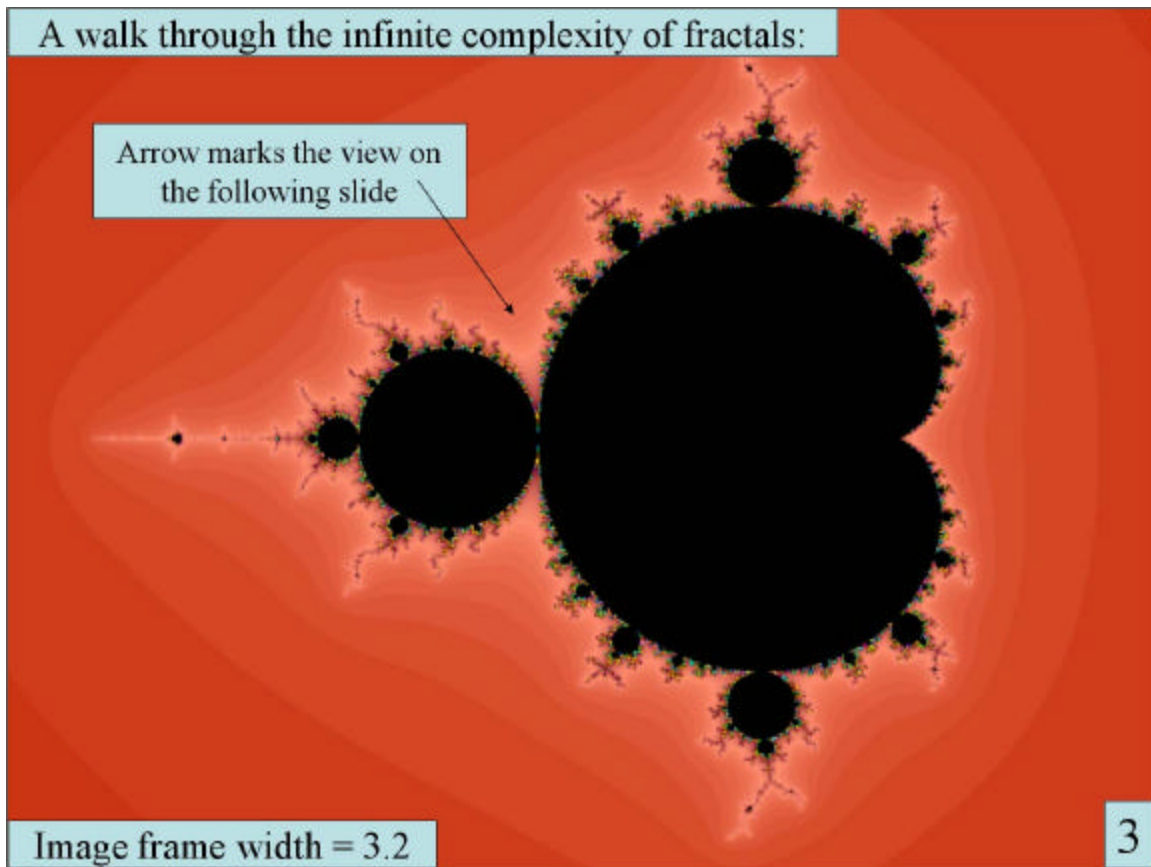
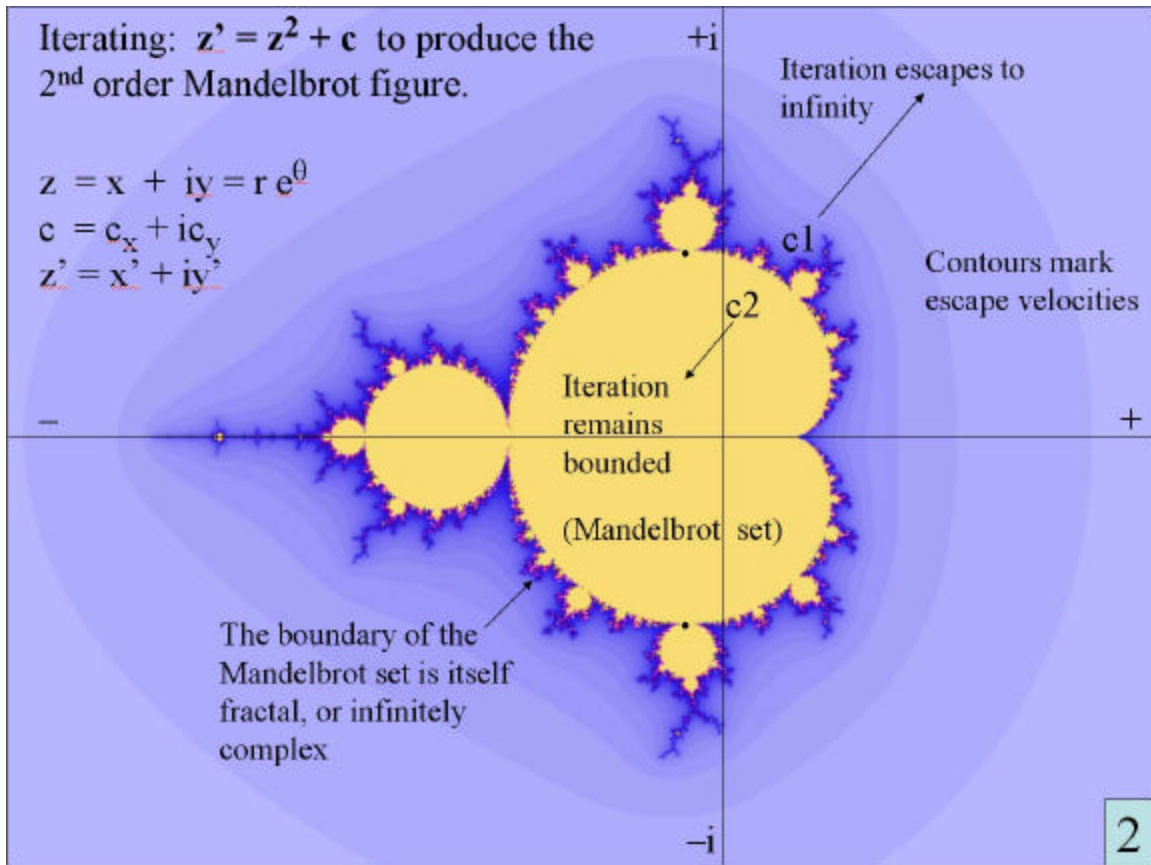
1. The Basic Mandelbrot Set
2. The Infinite Complexity of Mandelbrot Fractals
3. Escape Radii and Scale Constants in 2nd Order Mandelbrots
4. Higher Order Mandelbrot Figures
5. Scale Behavior for Higher Orders
6. Iteration of Other Functions than z^n : Power Series and Fractal Order
7. Iteration of General Power Series
 - (a) z^3+z^2
 - (b) $z^6-z^4+z^2$
 - (c) $z^{10}-z^5-z^2$ and $(z^{10}-z^5-z^2)/(z^4+1)$
 - (d) $\sum n*z^n$ and $\sum z^n/n$ with n from 2 to 40
8. Application to Infinite Series and Higher Mathematical Functions
9. Synthesis of Higher Order Functions by Combining Power Series
10. The Natural History of Mandelbrot Figures

1. The Basic Mandelbrot Set

The Mandelbrot figure, and the concept of fractals in general, have become widely known since they were first proposed by Benoit Mandelbrot and others (1-5), and subsequently developed by H. O. Peitgen and coworkers (6-8). It is amazing that figures of such beauty and literally infinite complexity could arise from very simple mathematical operations. The basic Mandelbrot figure, diagrammed in **Figure 2** and depicted in **Figure 3** is a plot on the complex plane, $z = x + iy$, of the results of iterating the equation:

$$z' = z^2 + c \quad (1)$$

where $z' = x' + iy'$ is the new location of a point on the complex plane; $z = x + iy$ is the previous point; and $c = c_x + ic_y$ is a selected starting location on the plane. Depending on the choice of c , the points produced by successive iterations of Equation 1 will either (a) move off to infinity, (b) migrate to zero or some other fixed point or points, or (c) cycle around the same set of repeated values forever. All starting points, c , which do not ultimately iterate to infinity are defined as the Mandelbrot set, and these points are black in Figure 3. Points which iterate to infinity lie outside the Mandelbrot set, and are colored in Figure 3. Such a simple mathematical idea produces unexpectedly intricate results. All points within the Mandelbrot set are connected, and the border separating the set from the outside is infinitely complex; it is, in fact, a fractal boundary.



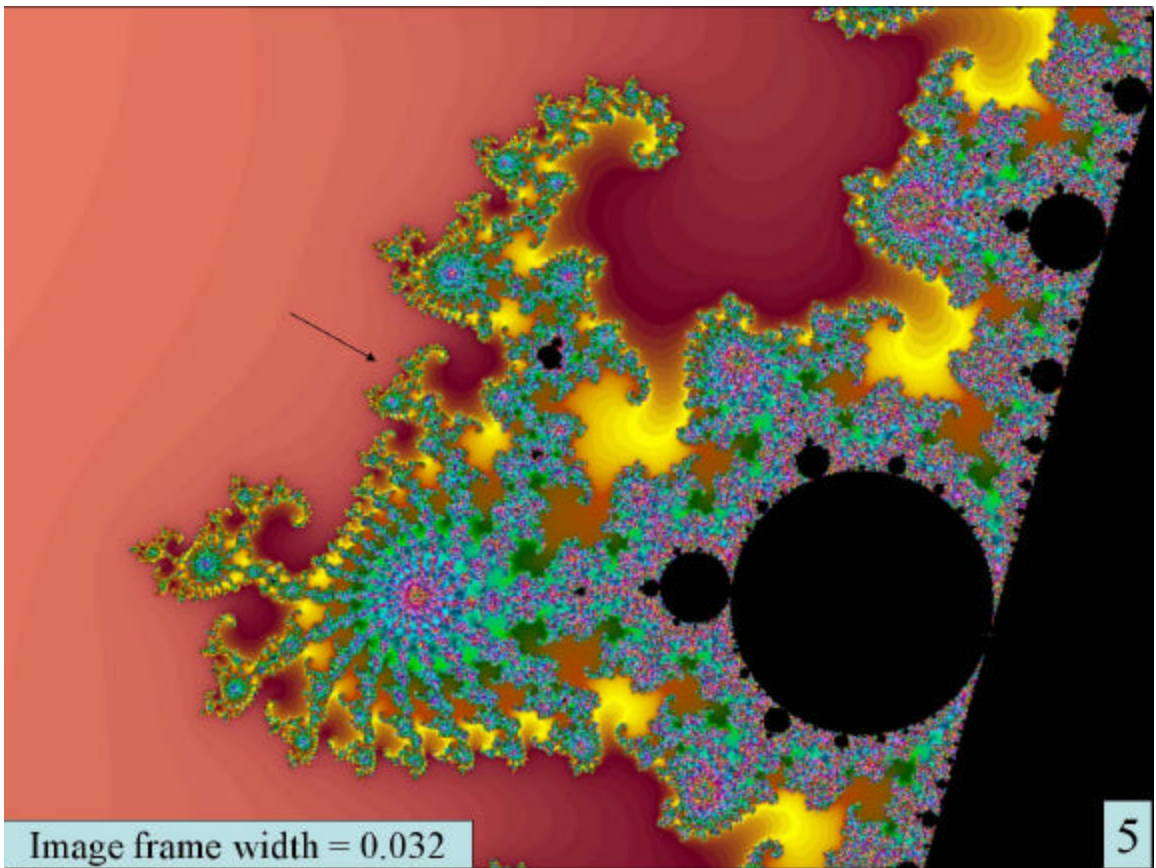
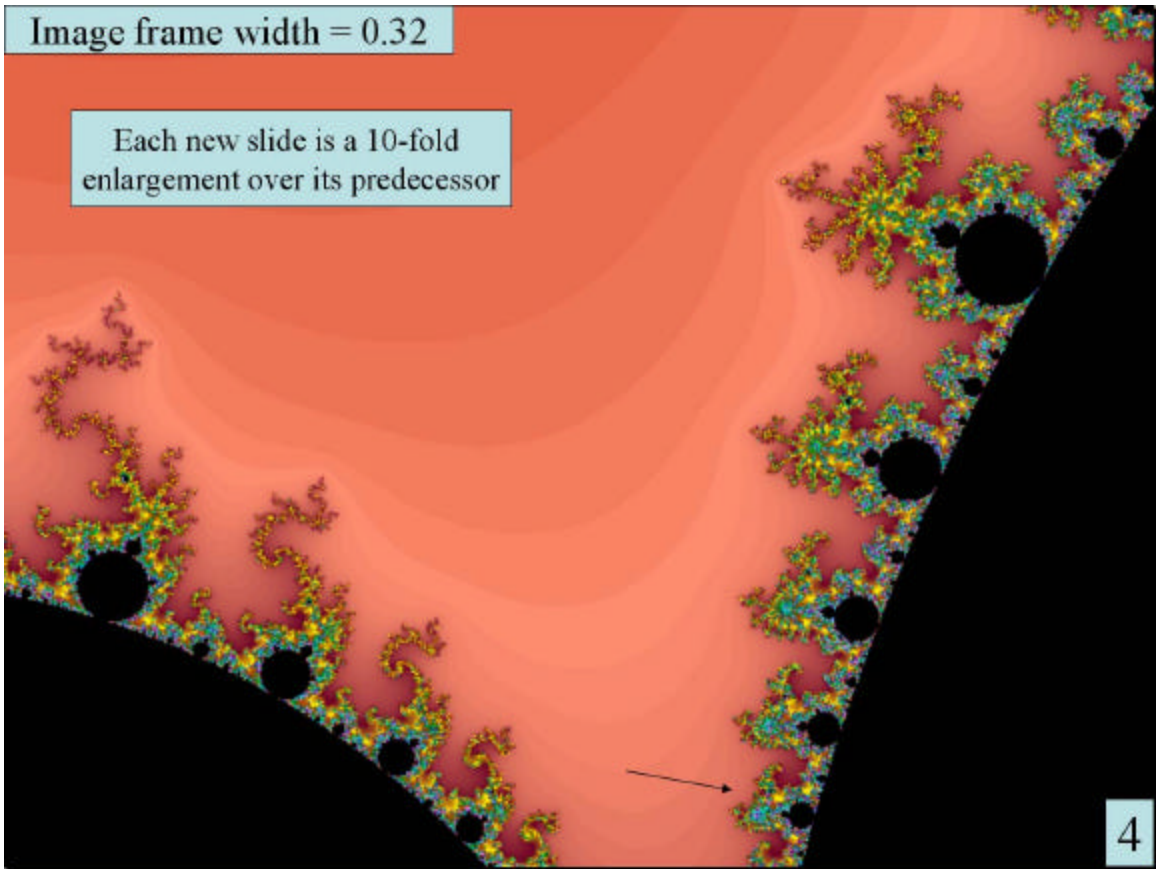
The z^2 Mandelbrot plot has been popularized in the technical and non-technical literature and is thoroughly familiar. But what happens if the iteration formula of Equation 1 is made more complicated—if higher powers of z are used, or other functions of z such as $\sin(z)$ or e^z or $\ln(z)$? That is the subject of this paper. Results presented here have been verified by comparing the output of two versatile fractal programs described in the Appendix: Dennis C. De Mars' *Fractal Domains* (FD) and Peter Stone's *Fractal Explorer* (FE). This is an experimental and descriptive analysis of fractal behavior, rather than an attempt to derive behavior theoretically from first principles. It is the work of an *amateur* in the original Latin meaning of the term: a *lover* of the mathematics and the relationships therein. If it can create a similar love of fractal behavior in the reader, it will have achieved its purpose.

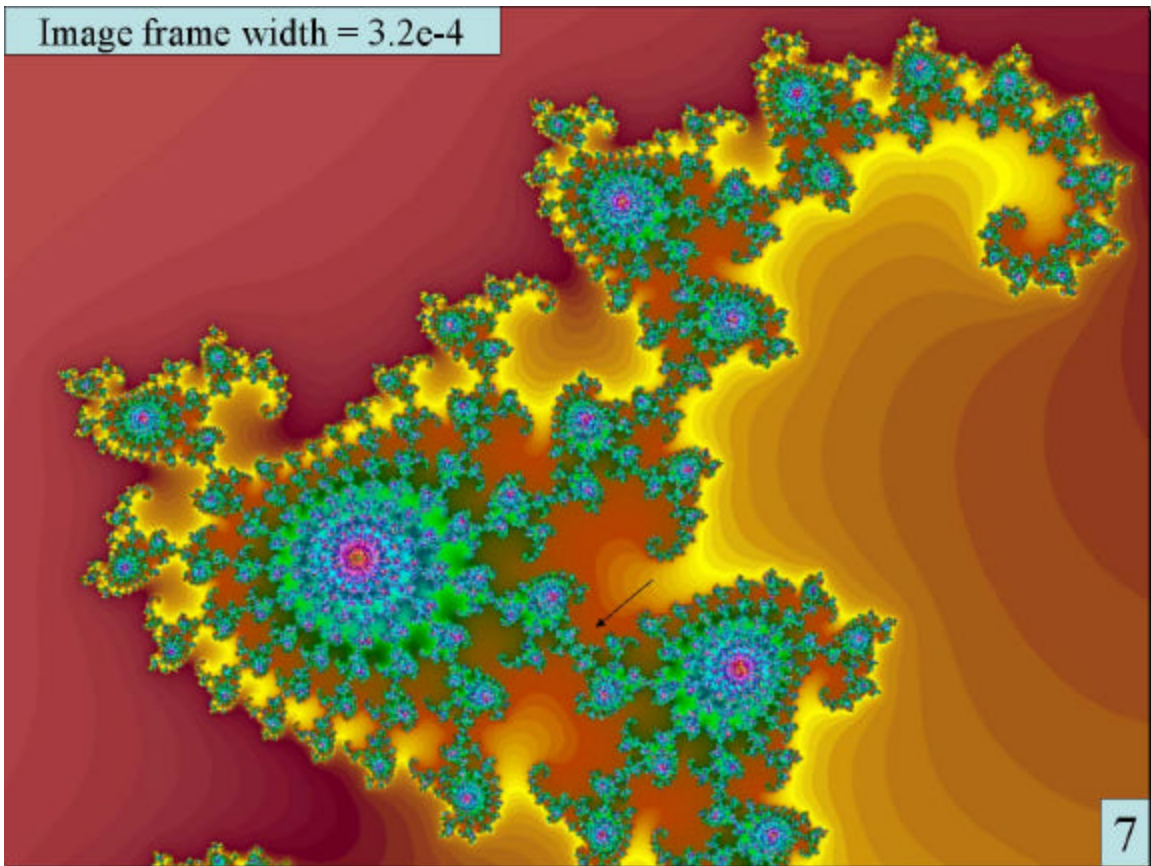
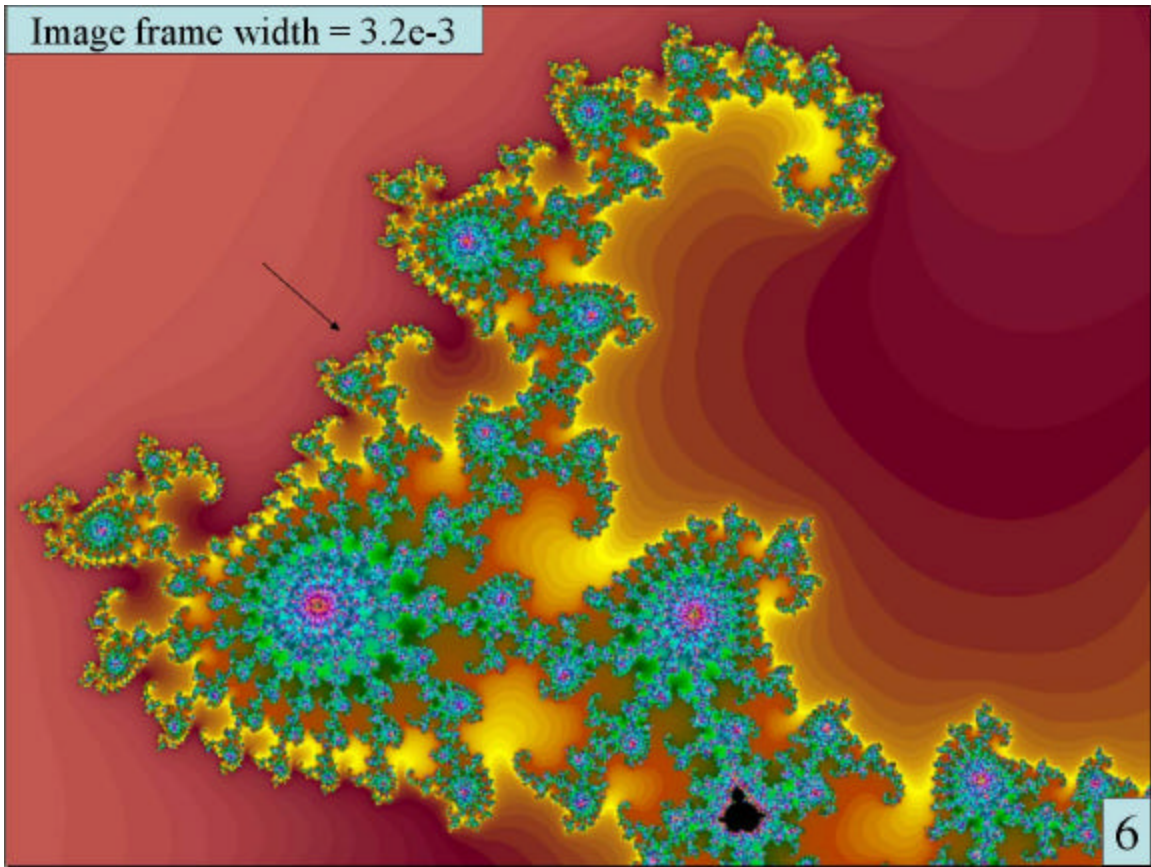
2. The Infinite Complexity of Mandelbrot Fractals

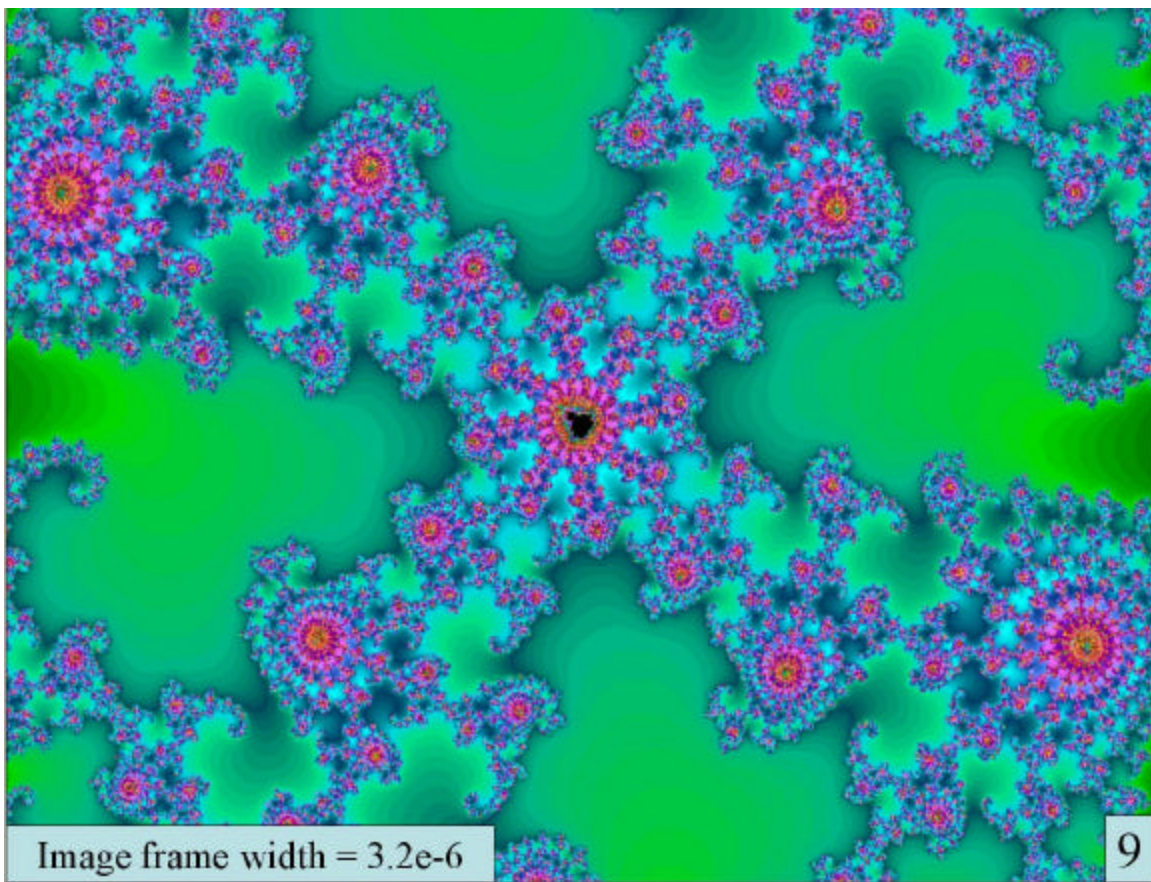
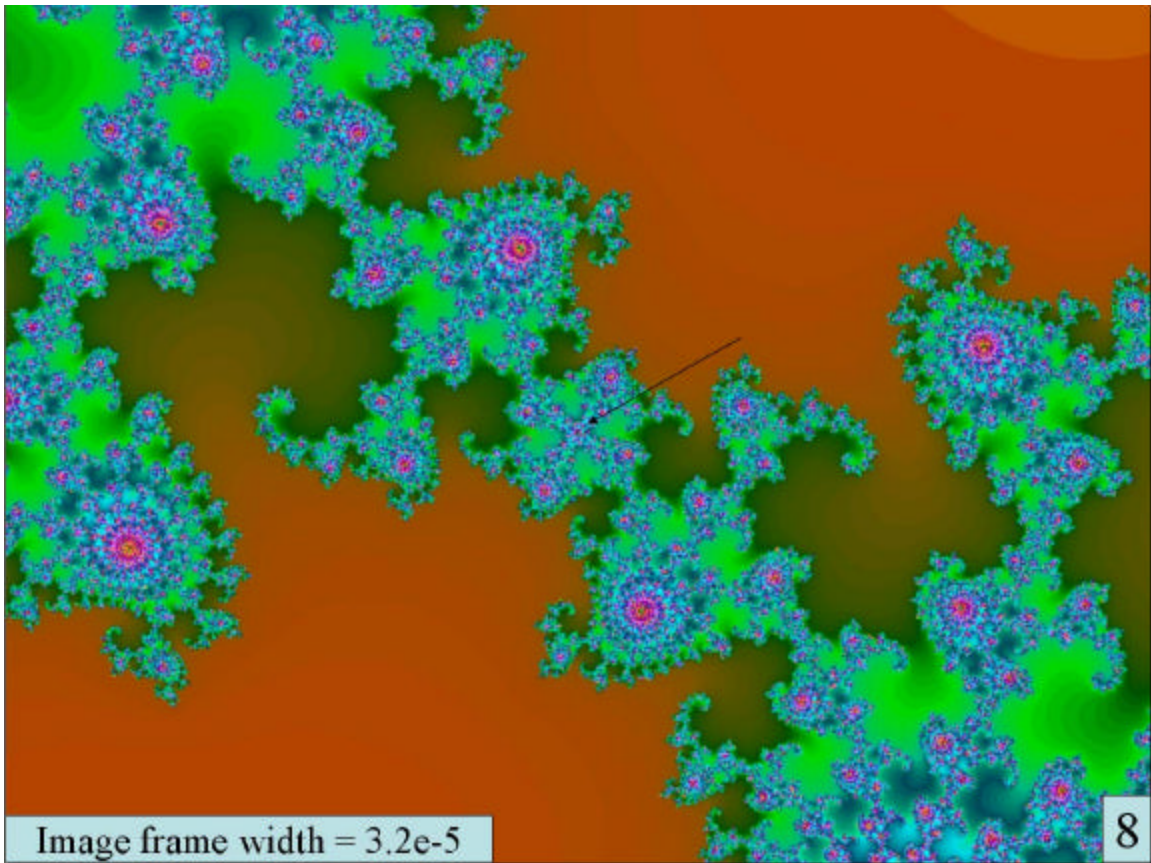
A defining property of fractals is that, upon magnification, they are seen to be self-identical or at least self-similar. The familiar 2nd order Mandelbrot of Figures 2 and 3 has a large pear-shaped central body, with one major lobe pointing to the left in the $-x$ direction, smaller lobes above and below, and a cusp or junction between two halves of the main body to the right. Its entire boundary is ringed by secondary lobes. These secondary lobes, if examined carefully, are seen to be ringed by even tinier lobes, and those are bordered by microscopic lobes in their turn. Enlarging any given segment of the Mandelbrot boundary yields a boundary that is fully as intricate as the original, and the complexity extends to infinity. Indeed, that is essentially the definition of a fractal. In an oft-quoted paraphrase of Jonathan Swift:

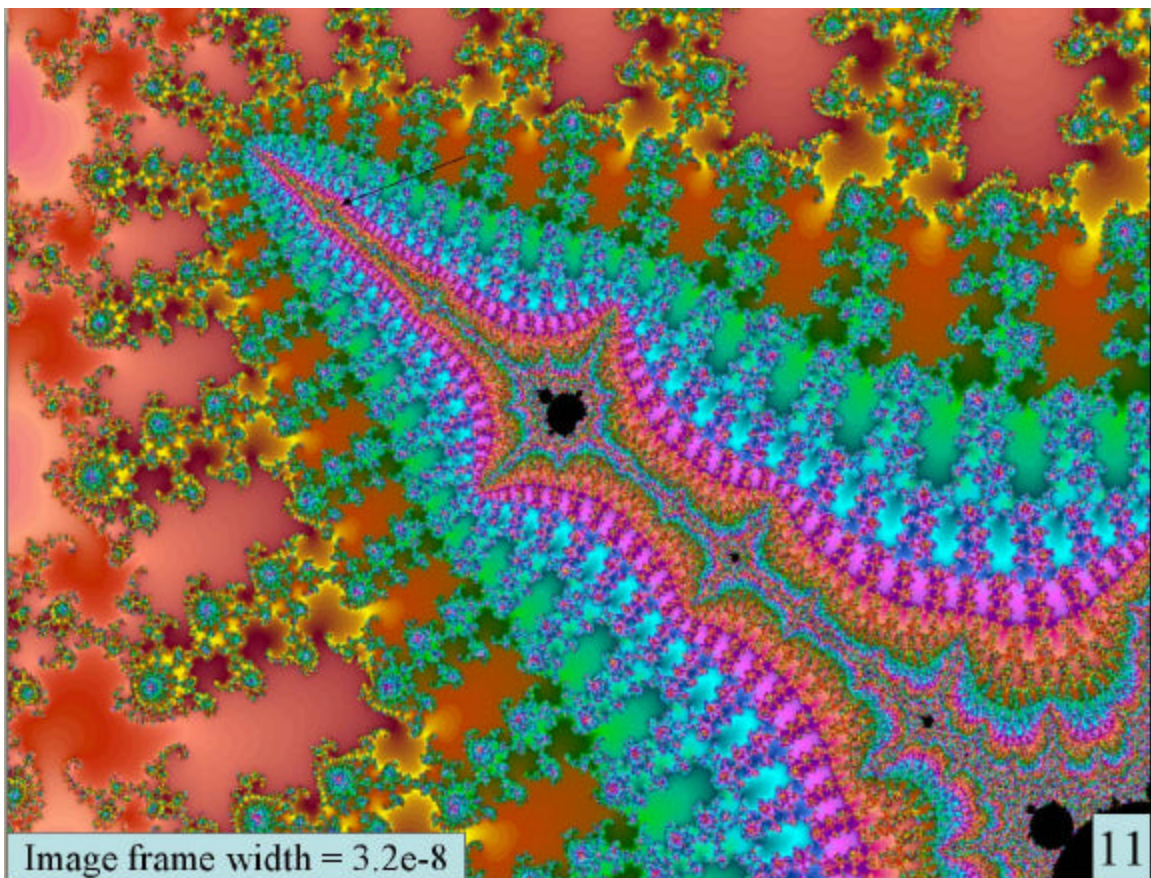
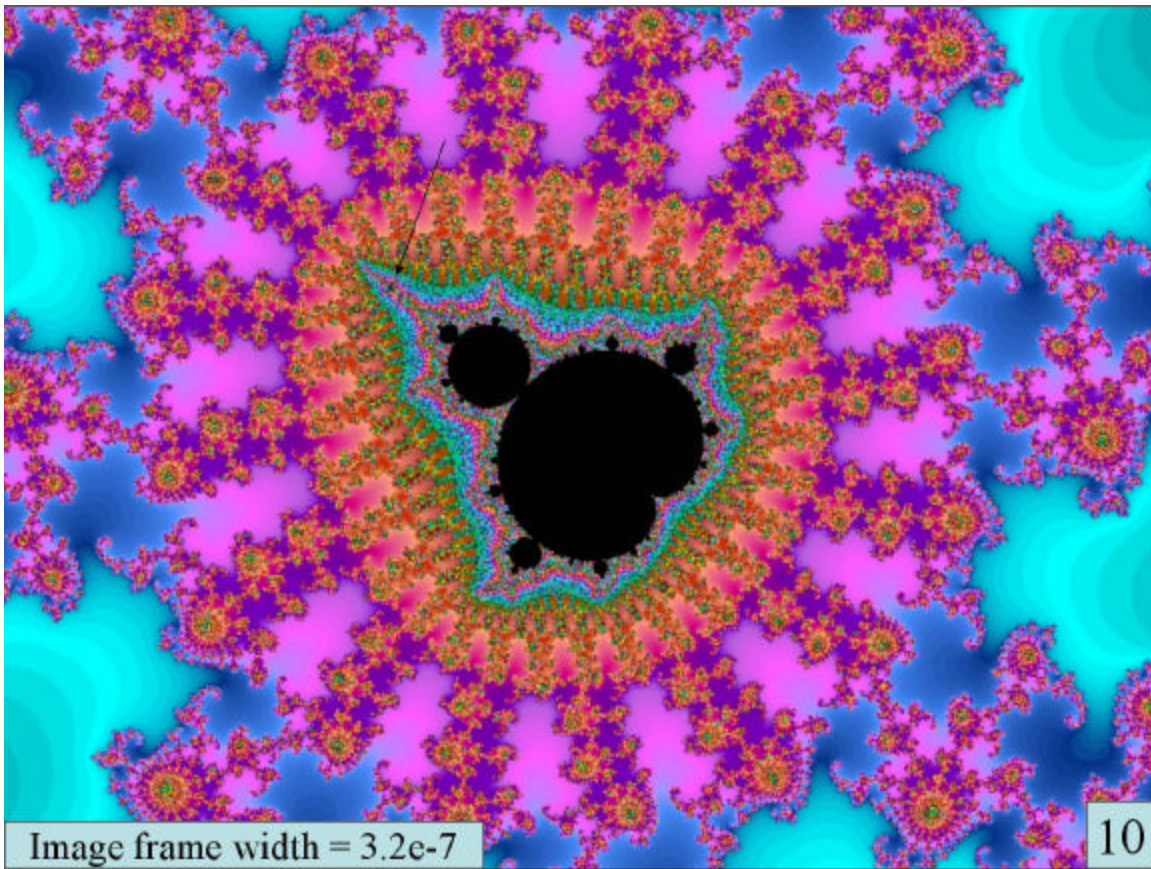
"Big fleas have little fleas, upon their backs to bite 'em,
And little fleas have lesser fleas, and so on *ad infinitum*."

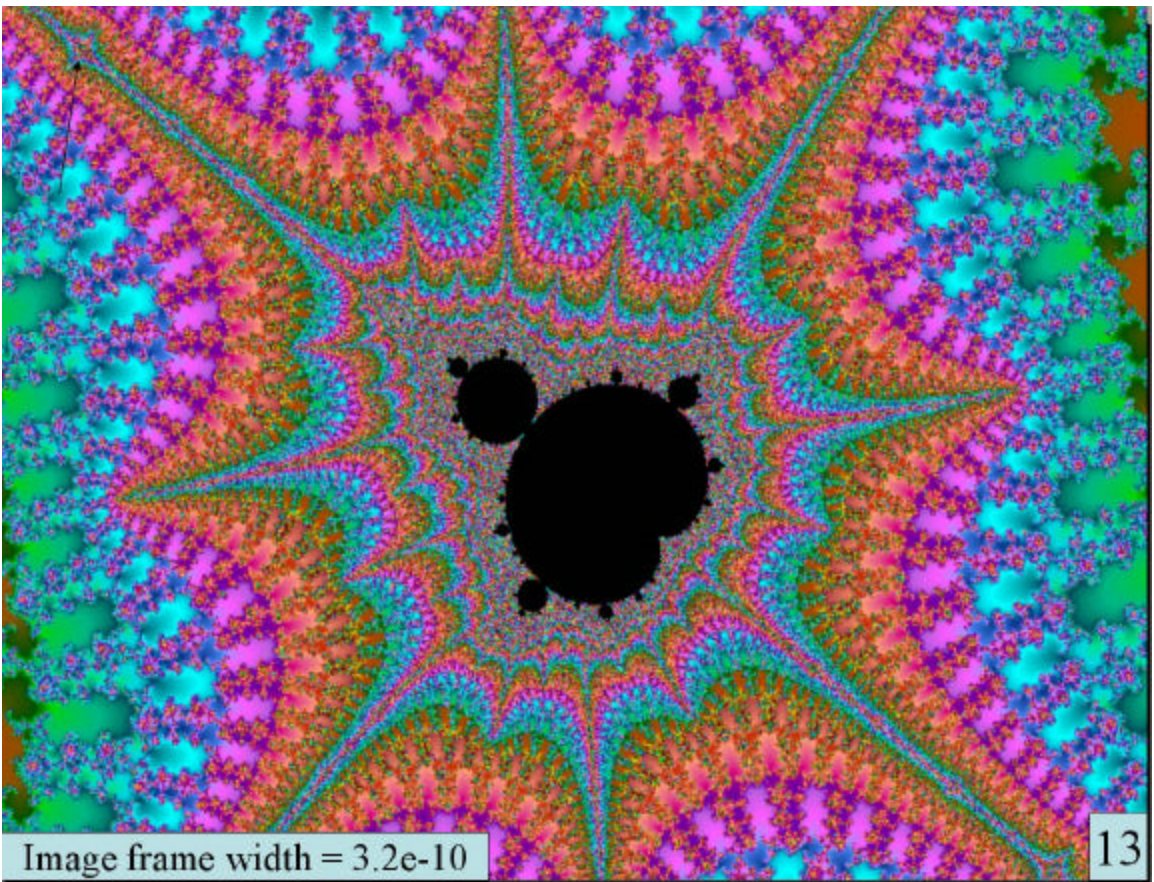
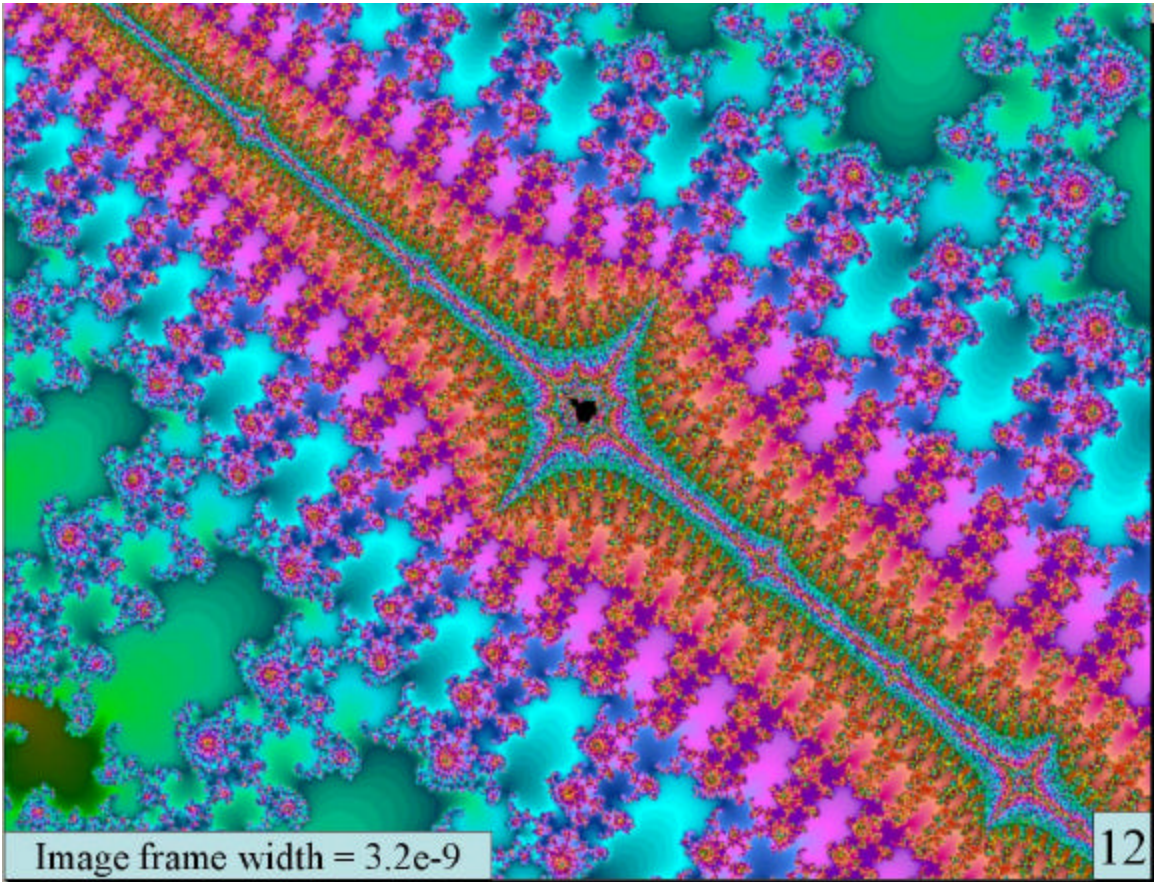
Figures 3–17 are a demonstration walk through fourteen orders of enlargement of the z^2 Mandelbrot, with tenfold magnification at each step. The overall shape of the starting body is mimicked by an infinite number of tiny replicas which can be seen at every level of magnification. When the process ends in a blur of rectangular pixels in Figure 17 after enlargement by a factor of 10^{14} or 100,000,000,000,000, the fault lies not with the fractal itself, but with the number of significant figures carried by the computer program and our willingness to wait for lengthy iterations. The complexity of the fractal itself has no limits. (As an aside, the enlargement factor of 100,000,000,000,000 seen here would convert one sixteenth of an inch into the distance from Earth to the Sun.)













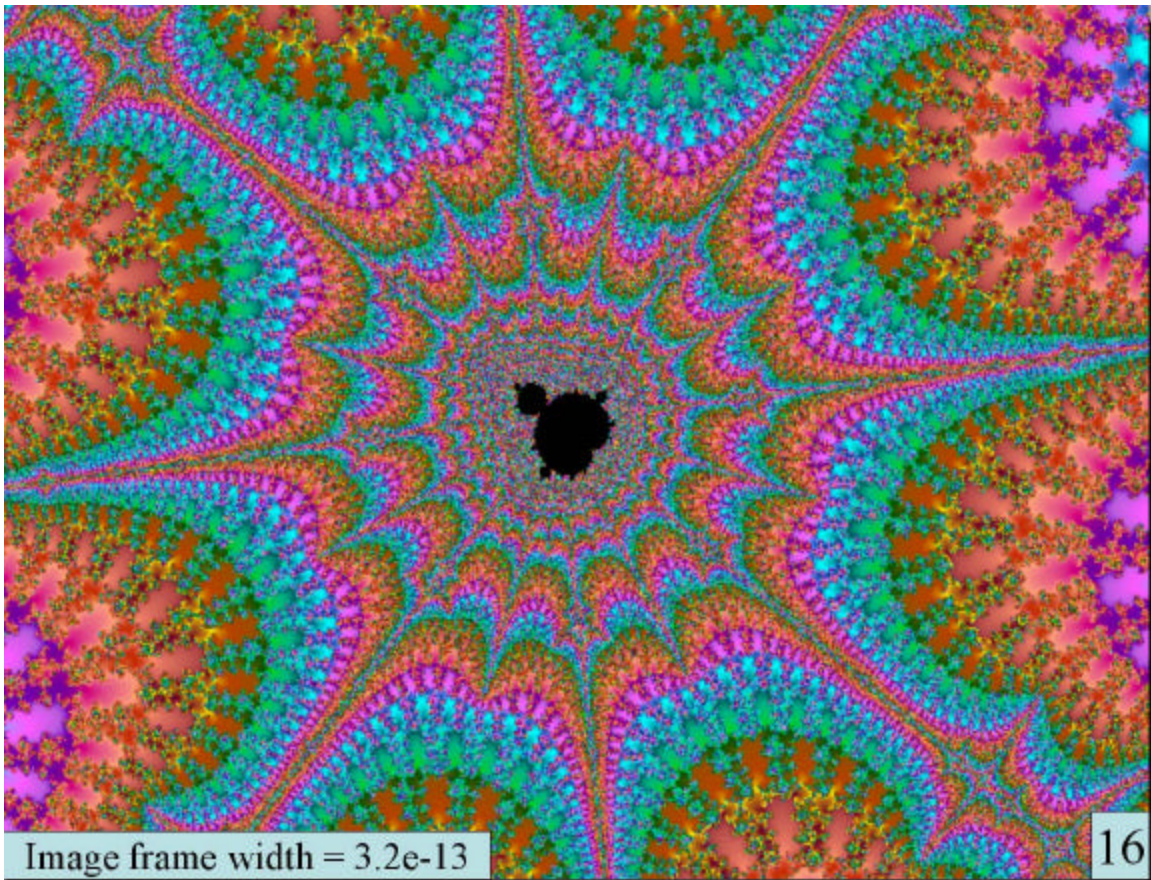
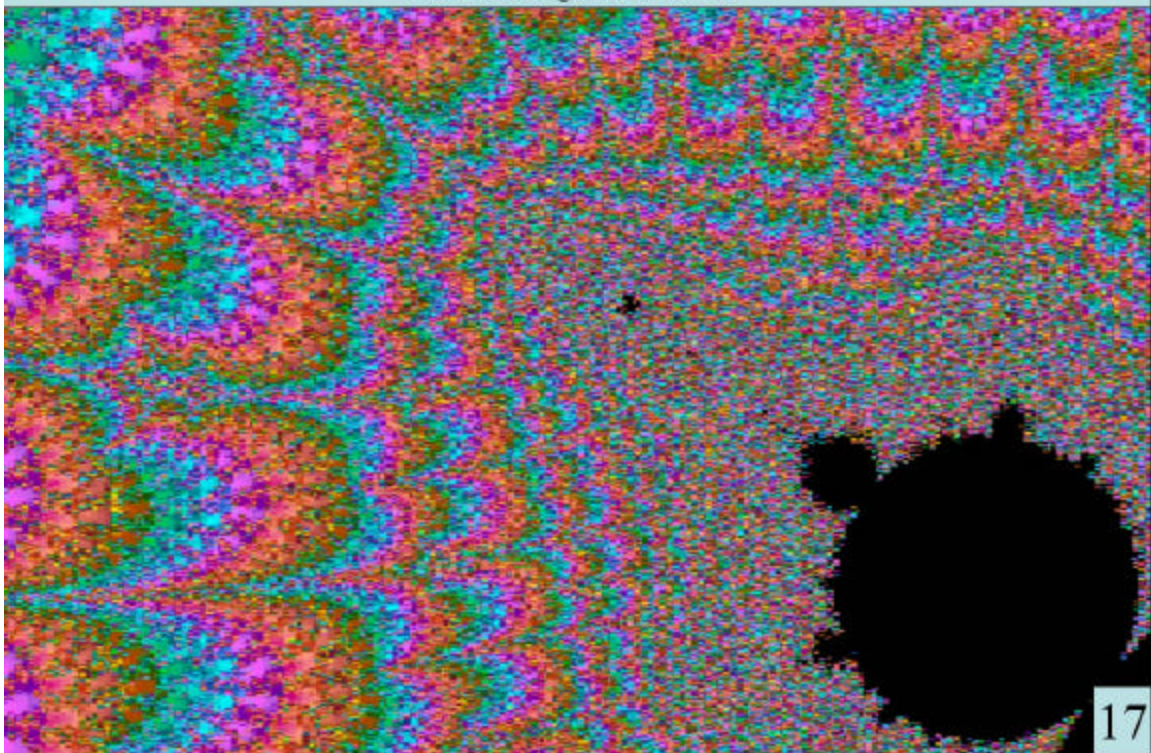


Image frame width = $3.2e-14$, or a total magnification of 100 million million. Visible pixels now blurring the image only indicate limitations of the computer program. The fractals go on forever.



Two key issues are addressed in this presentation:

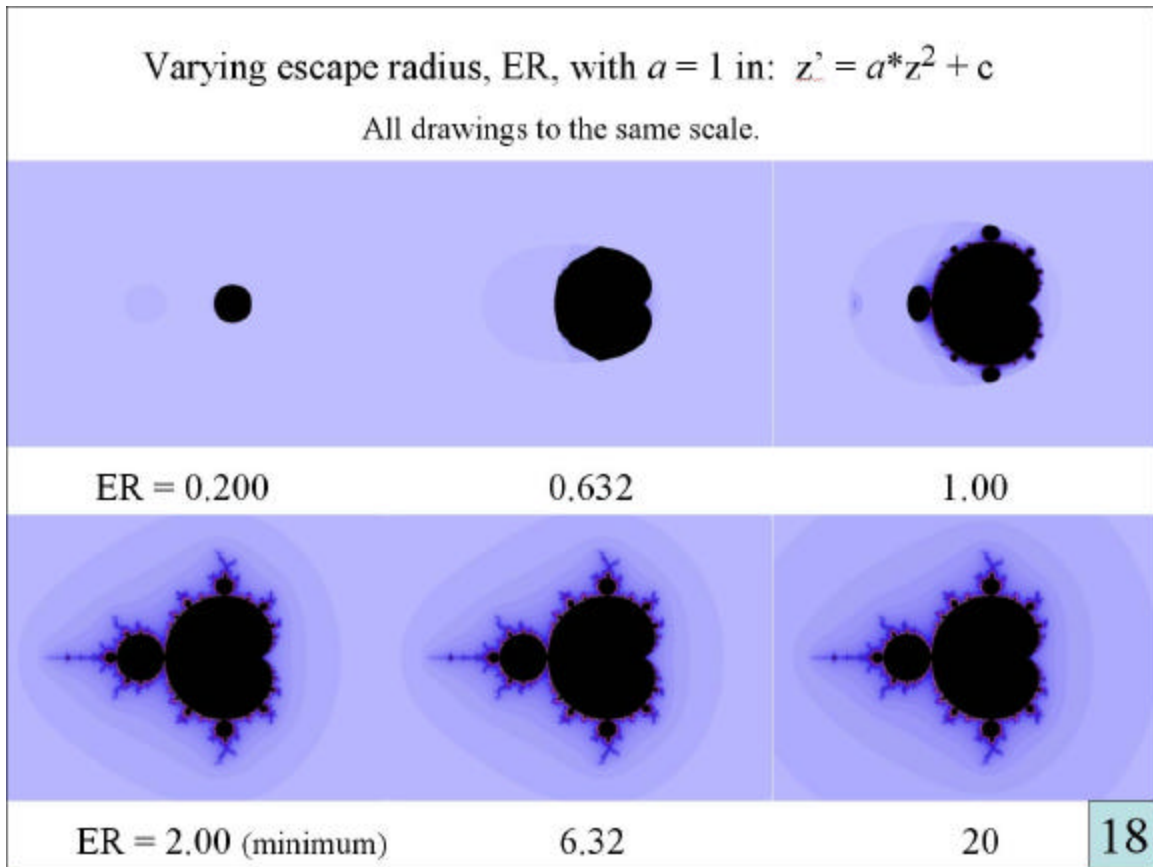
(a) Can one extend the basic Mandelbrot function to higher powers of z , and introduce a meaningful scaling constant? That is, can: $z' = z^2 + c$ be generalized to: $z' = a*z^n + c$?

(b) Can more general trigonometric or exponential functions $F(z)$ also be iterated via: $z' = a*F(z) + c$? If so, can one predict in advance how such functions will behave?

3. Escape Radii and Scale Constants in 2nd Order Mandelbrots

The ultimate test of whether a point on the xy plane is to be excluded from the Mandelbrot set is whether it iterates to infinity, given an infinite number of iteration cycles. An infinite number of cycles is not computationally practical, and so a compromise is used: a point is excluded from the Mandelbrot set if during a certain number of cycles it has moved farther than a preset distance termed the *escape radius*, ER . It can be shown that any point which moves past $|z| = 2.00$ will eventually escape to infinity, so the minimum acceptable escape radius for iteration with Equation 1 is $ER_m = 2.00$.

Figure 18 shows the results of iterating Equation 1 using various choices of escape radius. An ER of 2.00 or greater yields a mature 2nd order Mandelbrot figure which remains invariant in both size and shape as ER increases still further. But if one chooses an ER less than 2.00, then one is concluding erroneously that all those points in the Mandelbrot figure that extend outside the ER limit are in fact escape points, and not a part of the Mandelbrot set. The residual figure becomes more and more inaccurate and misshapen as ER falls, as though the constricted radius were drawing a noose about the mature figure. At $ER = 1.00$ the outermost details of the mature figure have been smoothed away. At $ER = 0.632$ all features have been eliminated except for an indentation at the right. For $ER = 0.200$ or less, only a smooth, featureless disk remains, of radius equal to ER . In summary, below the critical minimum ER_m value one has only a partial figure, that which lies within a circle of radius ER . For $ER = ER_m$ a complete Mandelbrot figure is seen, which is independent of the precise value of ER .



What happens if one iterates Equation 1 with an additional scale factor, a ?

$$z' = a*z^2 + c \quad (2)$$

If during subsequent iterations each successive z' is enlarged by a factor, a , then the threshold escape radius need only be $1/a$ of its previous value, or:

$$ER_m = 2/a \quad (3)$$

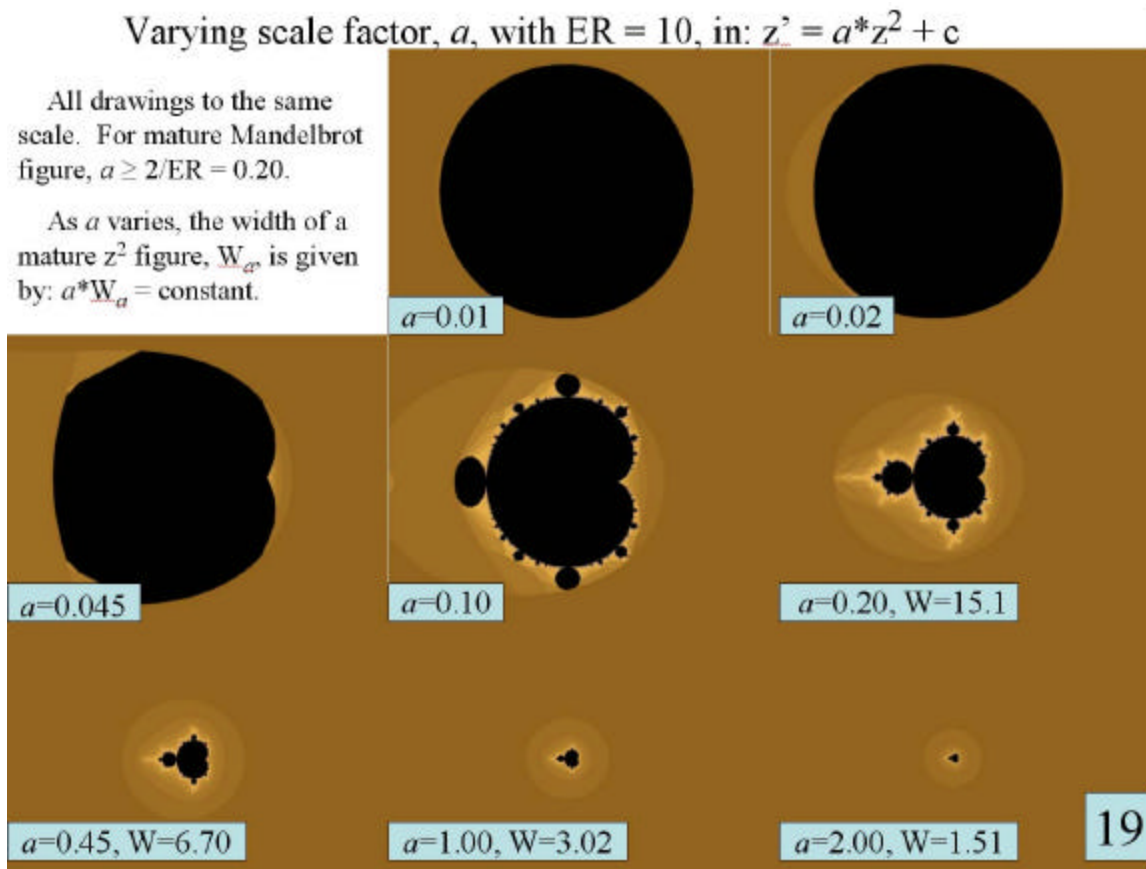
In addition, the size of the mature 2nd order Mandelbrot figure decreases as a increases. If W_a is some consistent measure of the width of the figure, then:

$$a*W_a = \text{constant} = K \quad (4)$$

Throughout this paper, a capital W_a will indicate the width of a Mandelbrot figure itself at a particular value of a , whereas a lower case w will represent the width of the image frame, as a measure of relative magnifications. For a 2nd order Mandelbrot, the most dependable dimension is its width measured up and down the imaginary axis, avoiding the long spine pointing to the left.

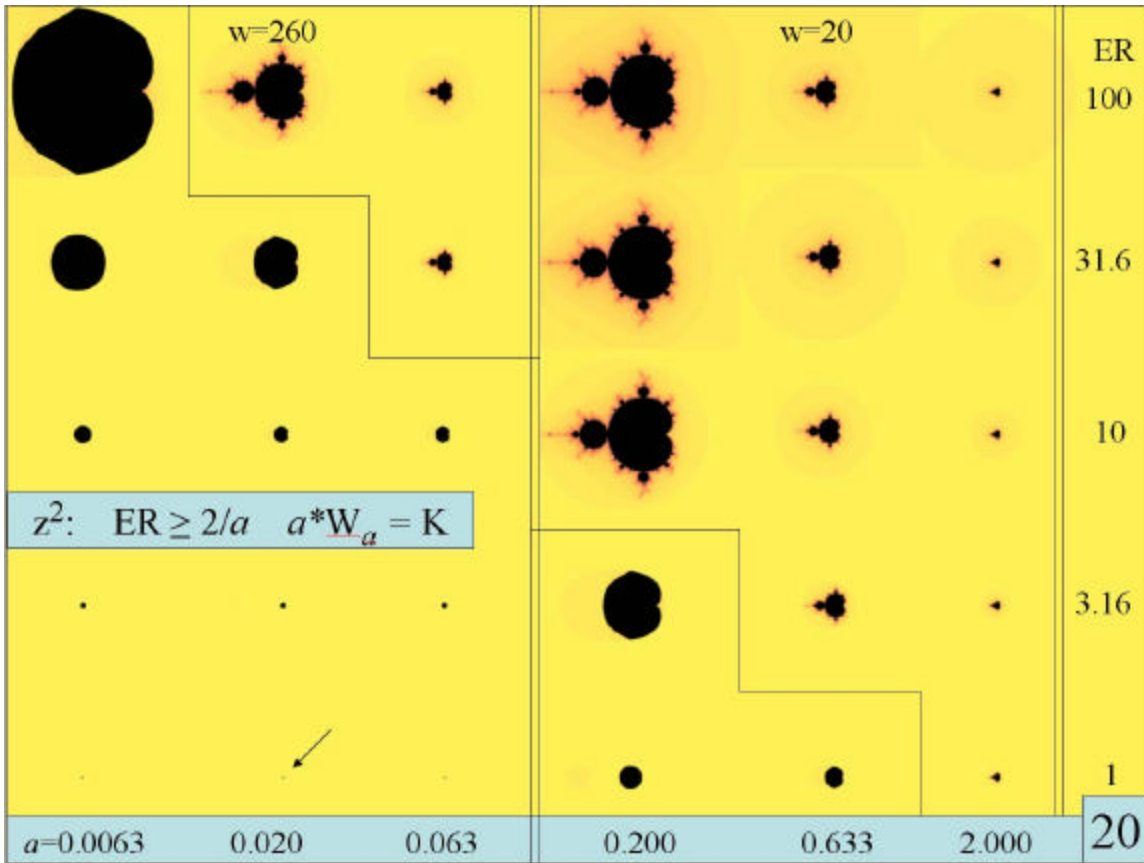
Figure 19 illustrates two features: the way the Mandelbrot image expands according to $a*W_a = K$ as a falls, and the way the image begins to degrade when a sinks below the threshold of $a = 2/ER$. ER is fixed at 10 while a is varied from

2.00 down to 0.01. With $ER=10$ the critical transition occurs at $a = 2/ER = 0.20$. Above this point a mature Mandelbrot results, of width decreasing linearly according to Equation 4. Below $a = 0.20$ one sees the expected planing away and smoothing of the figure, leading to a featureless residual disk by $a = 0.02$.



A graphic way of thinking about what is happening is that, as a decreases, the mature Mandelbrot figure in this example expands according to Equation 4 until it touches the perimeter of radius $ER = 10$ when $a = 0.20$. As the figure tries to expand still further at lower a , it clashes with the limiting circle and is deformed. The features seen in Figure 19 below $a = 0.20$ are not independent objects; they are incomplete, deformed Mandelbrots. That for $a = 0.10$ can be restored to its mature form by increasing ER to 20 so that once again: $a*ER_m = 2$. Even the featureless disk at $a = 0.01$ can be given its full mature form by increasing ER from 10 to 200, again making: $a*ER_m = 0.01*200 = 2$.

Figure 20 summarizes this behavior by comparing Mandelbrot images at six different a values (horizontal) and five different escape radii (vertical), in intervals of the square root of ten for convenience. For $ER = 1$ the Mandelbrot figure begins its collapse when a falls below 2.00. The integrity of the figure can be restored by increasing ER to 3.16, but failure again occurs when a falls below 0.633. Increasing ER to 10 yet again saves matters temporarily, but only to the point where $a = 0.200$. This stepwise correction process can be continued through $ER = 3.16$ to 100 and beyond. A mature Mandelbrot figure can be obtained at any value of a , no matter how small, by making the escape radius sufficiently large.



All images in Figure 19 are at the same scale. The first three columns in Figure 20 have a common scale, with a frame width of $w = 260$. But the last three columns have been enlarged by 13 times ($w = 20$) in order to show details. The zig-zag boundary separates mature Mandelbrots from their incomplete manifestations below the $ER_m = 2/a$ threshold. Note that below the threshold the size of the incomplete Mandelbrot figure *depends only on ER* and not upon a . But above this threshold the size of the mature figure *depends only on a* according to: $a \cdot W_a = K$, and is independent of escape radius.

4. Higher Order Mandelbrot Figures

Higher order Mandelbrot figures are obtained by iterating the expression:

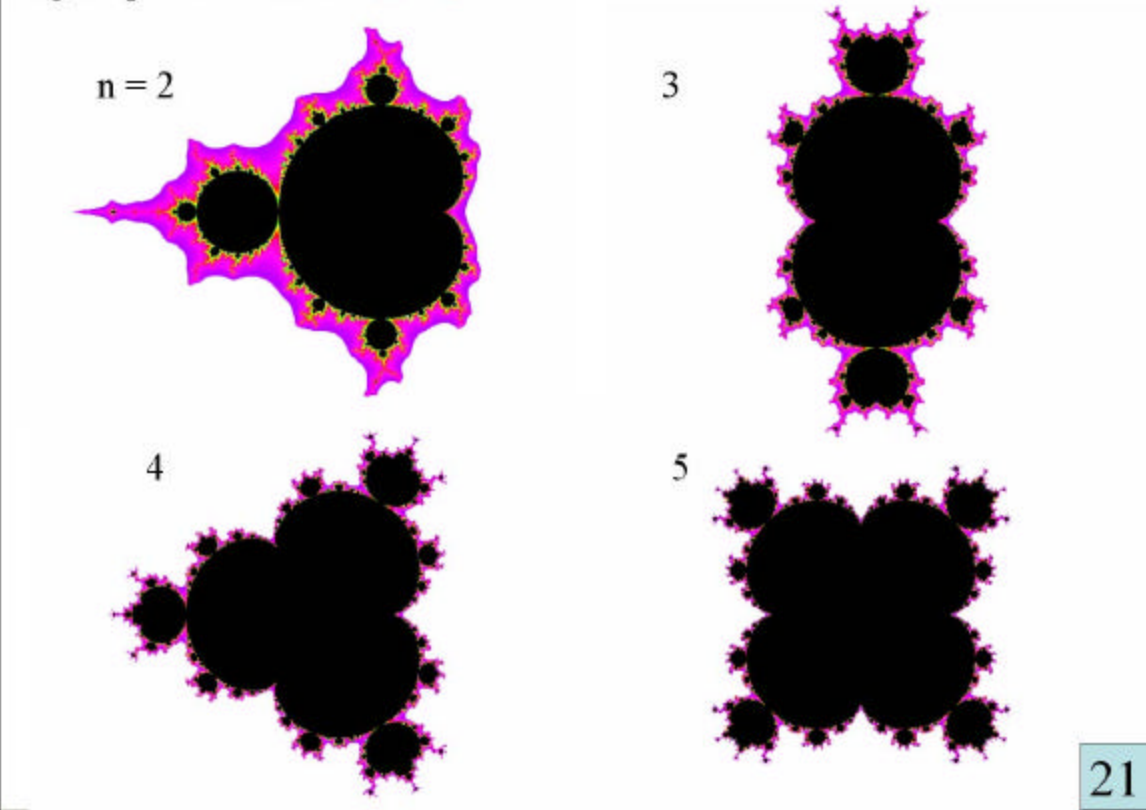
$$z' = a*z^n + c \quad (5)$$

where n is the *order* of the equation. Results for $a = 1$ and increasing values of n are shown in **Figures 21–22**. The Mandelbrot figure for $n = 3$ has two primary lobes extending up and down the vertical imaginary axis, and two incursive cusps or junctions to left and right along the horizontal real axis. It is surrounded as before by an infinitely complex set of smaller and smaller features. The figure for $n = 4$ has three main lobes, one of which points in the negative real axis direction. That for $n = 8$ has seven peripheral lobes.

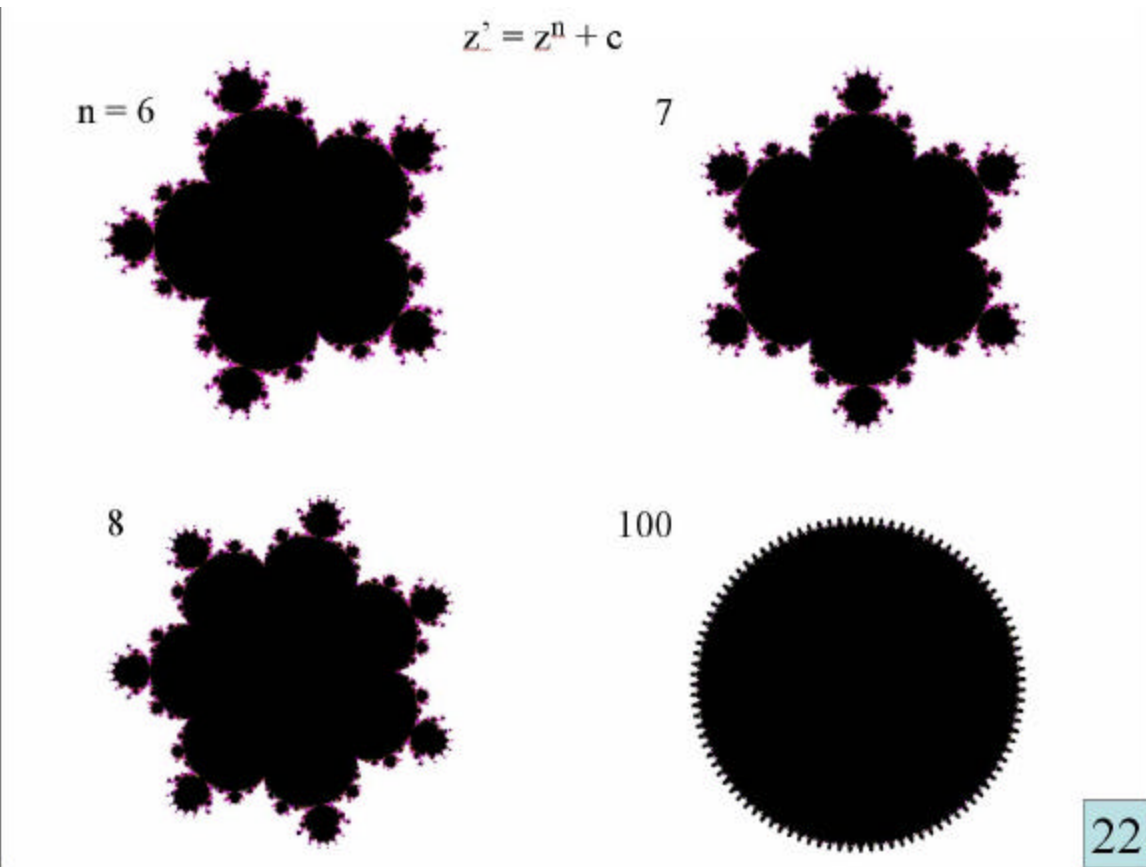
In general the iteration of Equation 5 with an exponent n yields an n^{th} order Mandelbrot figure displaying $n-1$ primary lobes around a central body, separated by $n-1$ incursive junctions. For odd n , with an even number of lobes and junctions, two of these junctions face right and left along the real axis. For even n , one of the odd number of lobes points to the left in the negative real direction.

Figure 22 also shows an extreme case of iterating z^{100} to produce a disk with 99 lobes. Each of those lobes, when magnified, shows the infinite complexity expected from a fractal figure by the Swift principle enumerated above. The set depicted in Figures 21–22 will be a standard for comparison with more complex functions, and will be termed "ideal n^{th} order Mandelbrot figures".

Higher powers of z in: $z^n = z^n + c$

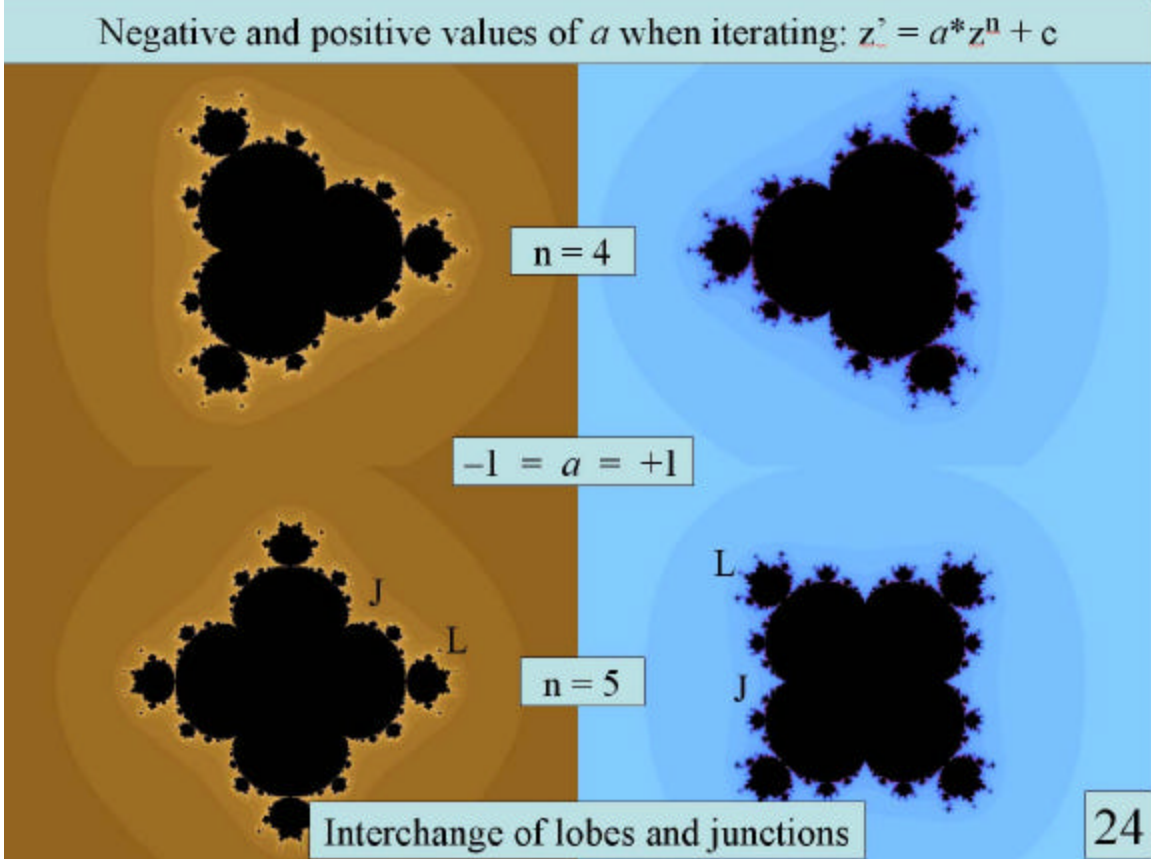
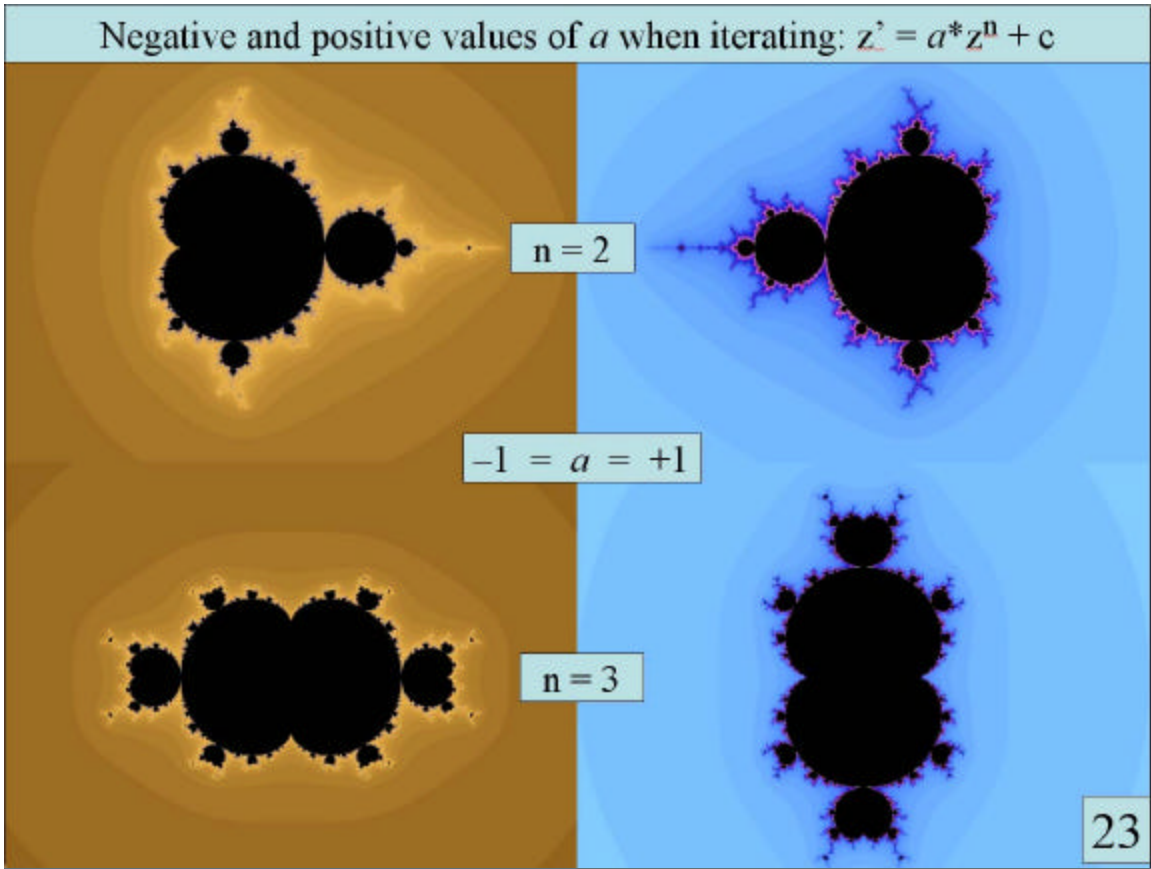


21



22

The constant a in Equation 2 is not limited to positive values. If the first term in the iteration expression $z' = a*z^n + c$ is negative, then the results are as shown in **Figures 23–24**. Now lobes rather than junctions face right and left for n odd (e.g.: 5), and the figure for even n (e.g.: 4) extends a lobe to the right with a junction at the left. One could think of the behavior with n even as a left/right reversal, and that for n odd as a rotation by $180^\circ/(n-1)$. But the simplest and most systematic description is one in which the intact figure is reoriented so that it interchanges positions of lobes (L) and junctions (J).

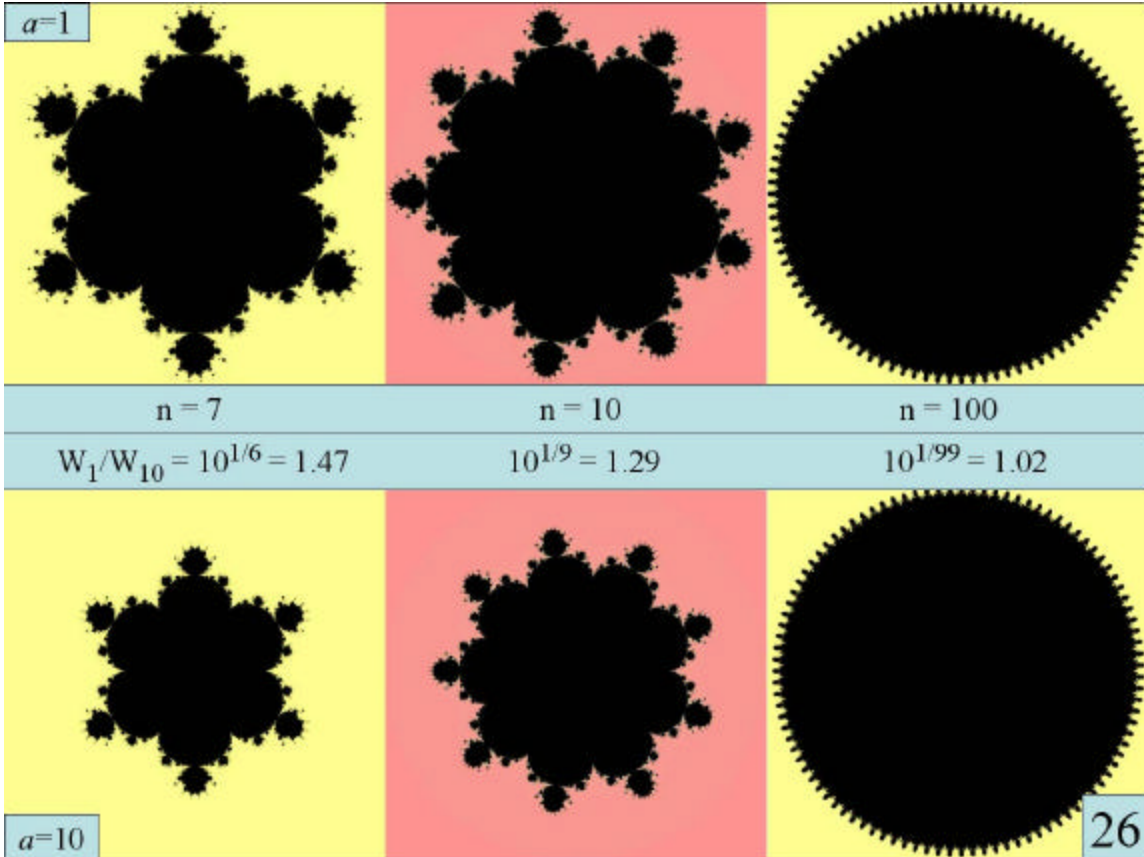
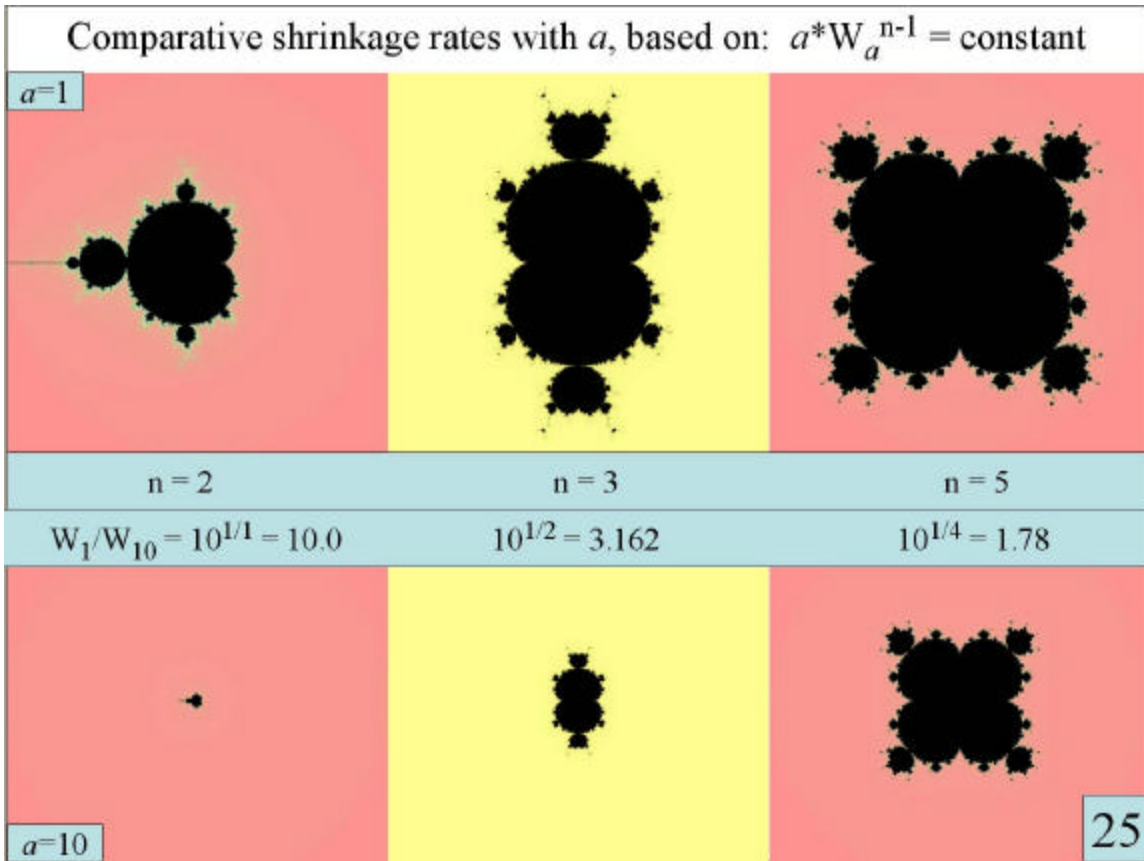


5. Scale Behavior for Higher Orders

Higher order z^n Mandelbrots also shrink when scale constant a increases, but less rapidly than 2nd order. **Figures 25–26** compare image sizes after tenfold increase in a value, for representative orders between 2 and 100. The higher the order, the slower the rate of shrinkage with a . The behavior of a n^{th} order figure is a generalization of the 2nd order expression with the image width W_a taken to the $(n-1)^{\text{st}}$ power:

$$a * W_a^{n-1} = K \quad (6)$$

This will be termed the *scale product equation*. It predicts that a tenfold increase in a leads to a shrinkage of the image by a factor of $W_a/W_{10a} = 10^{[1/(n-1)]}$. A 2nd order Mandelbrot shrinks by a factor of ten as a rises tenfold; and a 7th order by a factor of 1.47. But a 100th order Mandelbrot only diminishes by two percent in the same interval of a .



The general expression for threshold escape radius, ER_m , also is an extension of that for 2nd order. As before, the minimum escape radius is that which just fits snugly around the Mandelbrot figure, touching its outer features but not cutting them off. **Figure 27** shows closeups of the leftmost lobe of the z^4 Mandelbrot with $a = 1$, at three closely spaced ER values. For $ER = 1.30$ (right) the radius (orange circle) is too large to make contact with the Mandelbrot figure. For $ER = 1.22$ (left) it is too small, and some of the outermost spikes of the z^4 figure have been obliterated. Only for $ER = 1.26$ (center) does the z^4 figure make perfect touching contact with the escape radius circle, and this is precisely the value calculated for ER_m from Equation 7, a generalization of that for z^2 :

$$a \cdot ER_m^{n-1} = 2 \quad \text{or} \quad ER_m = (2/a)^{1/(n-1)} \quad (7)$$

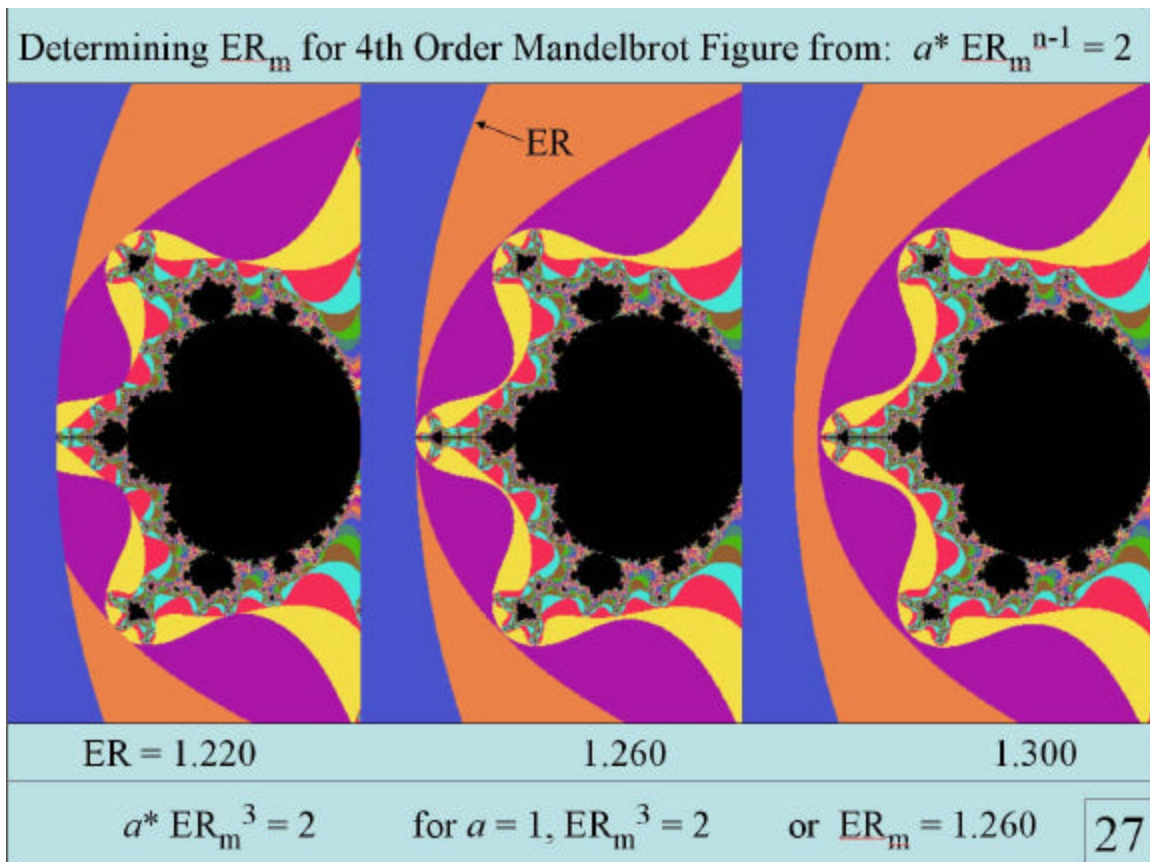
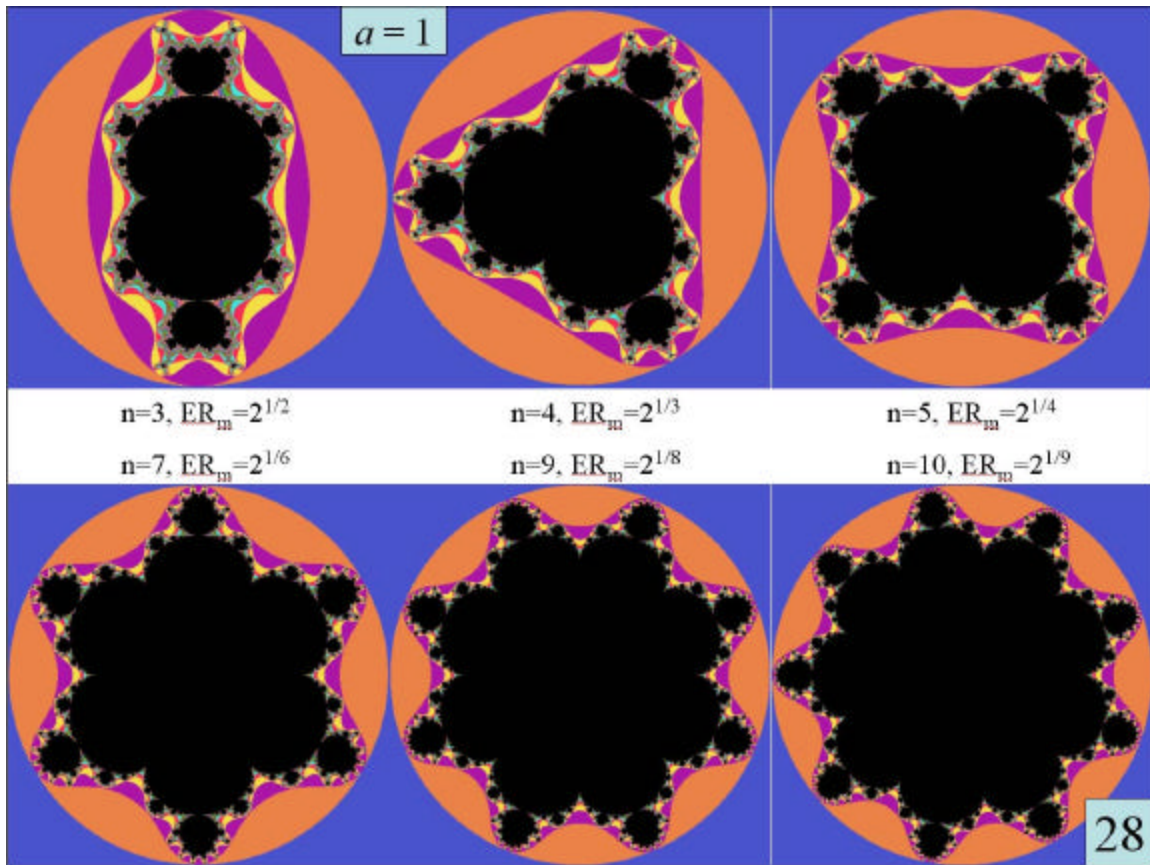
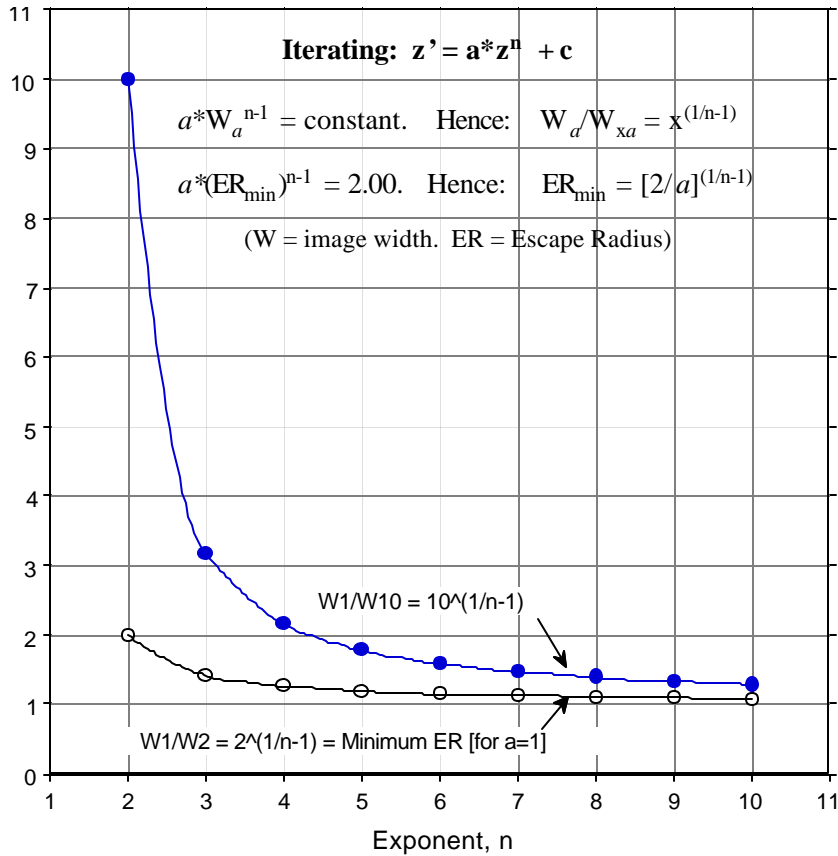


Figure 28 tests Equation 7 against higher order Mandelbrots from z^2 through z^{10} , with the escape radius drawn as an orange circle. In each case the figure has been drawn using the ER_m values derived from Equation 7, and in each case this choice just brings the radius into touching contact with the outer fringes of the Mandelbrot figure. For $a = 1$ the critical ER_m threshold for a 2nd order Mandelbrot had been at $ER = 2$. For 3^d order the threshold is $2^{(1/2)} = 1.414$, for 5th order it is $2^{(1/4)} = 1.19$, and for 10th order it is $2^{(1/9)} = 1.08$.

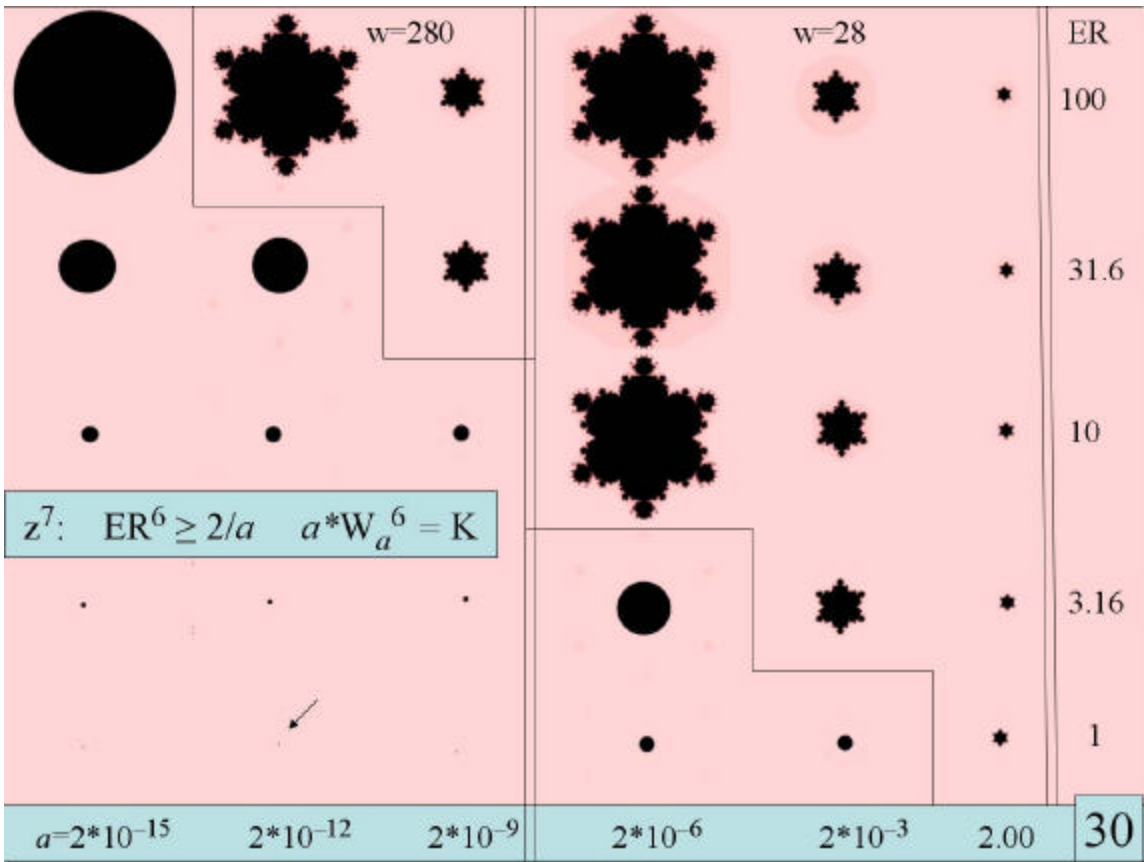


Shrinkage rates expressed as W_a/W_{10} and W_a/W_{2a} at $a = 1$ are plotted as a function of the order of iteration in **Figure 29**. Escape radius thresholds, ER_m , also are plotted. Note that the reduction factor for doubling of a has exactly the same form as the ER_m function at $a=1$, namely $2^{[1/(n-1)]}$.



29

The behavior of a 7th order Mandelbrot when ER and a are varied is shown in **Figure 30**. The three rightmost columns ($w = 28$) are enlarged over the first three ($w = 280$) by a factor of ten. The overall pattern is similar to that for 2nd order in Figure 20, except that the relevant minimum escape radius equation for 7th order is: $ER_m^6 = 2/a$, not: $ER_m = 2/a$. Hence the horizontal scale in a is greatly extended; for a given ER, the 7th order Mandelbrot figure remains intact to much lower a values than for 2nd order. This is because the 7th order image, by Equation 6, increases in size much more slowly as a falls, and only reaches the ER boundary radius at a considerably lower a value. Once again, below ER_m the size of the image *depends upon ER but not a* whereas above the threshold it *depends upon a but not ER*.



In sum, the shrinkage rate of mature higher-order Mandelbrot functions of the type z^n is given by Equation 6: $a * W_a^{n-1} = K$, and the minimum escape radius for a complete figure by Equation 7: $a * ER_m^{n-1} = 2$. Except for size, the same Mandelbrot figure is obtained at any a value above $a = 2/ER^{n-1}$. So it is indeed correct to maintain that for iteration of a single term z^n , a has no meaning other than as a scaling factor.

However, this is no longer true for even something so simple as the two-term power series z^3+z^2 . As we shall see below, for these series the scaling constant a does have a real effect, establishing which term of the power series exerts the most significant influence, and determining the changing shape of the resulting Mandelbrot figure.

6. Iteration of Other Functions than z^n : Power Series and Fractal Order

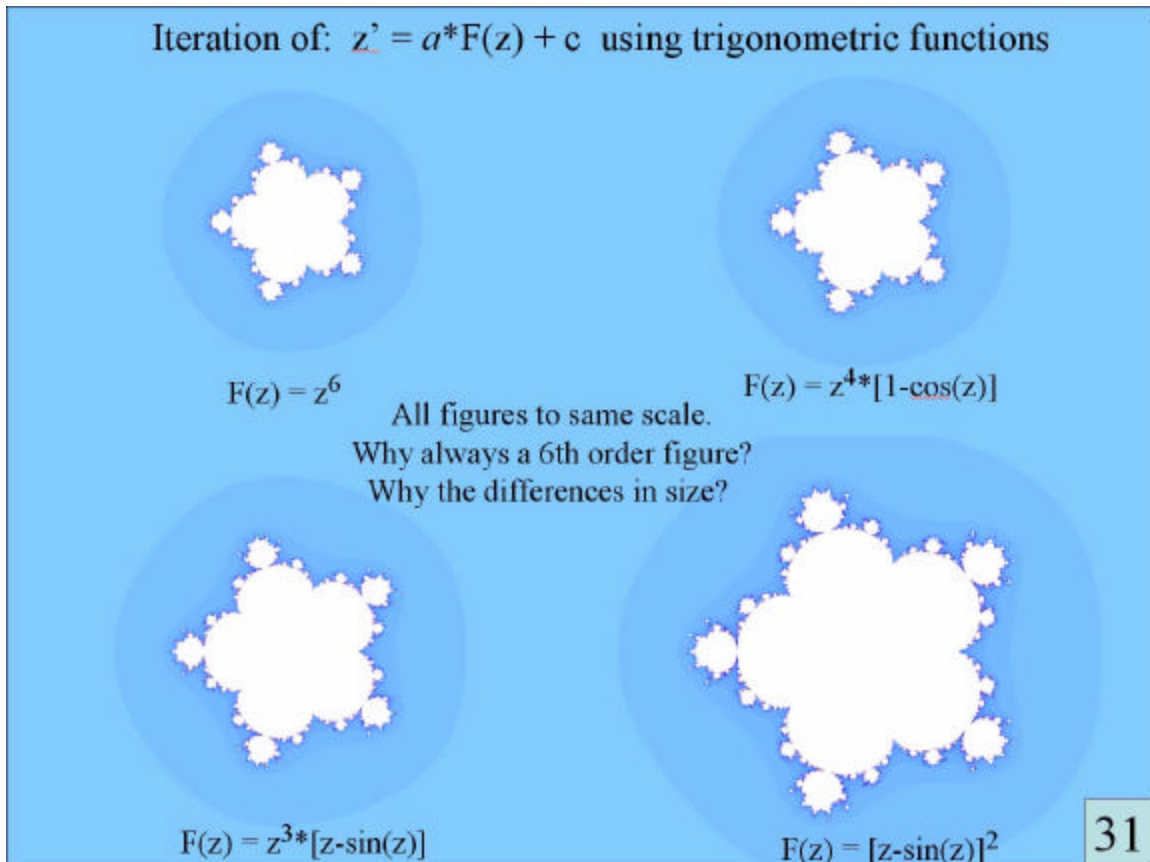
Iteration Equation (2) can be generalized to:

$$z' = a*f(z)*g(z) + c = a*F(z) + c \quad (8)$$

where $f(z)$, $g(z)$ and $F(z)$ are functions of z to be investigated. If both $f(z)$ and $g(z)$ are set equal to z , then the result is the basic 2nd order Mandelbrot of Figure 3. If both $f(z)$ and $g(z)$ are each set to z^3 (or to any powers such that the sum of their exponents is 6), then the result is the 6th order Mandelbrot seen at upper left of **Figure 31**. Moreover, an identical but slightly larger 6th order figure (upper right) results when $f(z) = z^4$ and $g(z) = [1-\cos(z)]$, suggesting that $[1-\cos(z)]$ in some manner has 2nd order properties. The function $[z-\sin(z)]$ appears to have 3rd order properties, as it yields a 6th order Mandelbrot figure when combined with z^3 . Indeed, this 3rd order property of $[z-\sin(z)]$ is verified by the observation that the same figure results when both $f(z)$ and $g(z)$ are set equal to $[z-\sin(z)]$, or when iterating:

$$z' = a*[z-\sin(z)]^2 + c \quad (9)$$

All images in Figure 31 are drawn to the same scale, and with $a = 100$ in order to ensure that each has its mature form.



In short, $[1-\cos(z)]$ can replace z^2 and $[z-\sin(z)]$ can replace z^3 in any Mandelbrot iteration. The shape of the iterated figure will be the same as that of simple z^n , where n is the sum of orders of the individual factors $f(z)$ and $g(z)$. Other functions and their fractal order will be considered below. In some cases the relevant n^{th} order Mandelbrot figure is not immediately evident at $a = 1.00$, and either larger a values or larger escape radii must be used to reveal it. In an anthropomorphic analogy, different functions with the same fractal order result in parent bodies that ultimately give birth to the same Mandelbrot figures, but at different values of ER and a . At ER = 10 the “point of birth” of a mature z^2 Mandelbrot figure is $a = 0.20$. For the 2nd order function $\tan(z) \cdot \arcsin(z)$ the birth point is around $a = 3.15$ and the image at $a = 1$ looks nothing at all like a 2nd order Mandelbrot. As a more extreme case, iteration of the function $\tan(z) \cdot (e^z - 1)$ does not produce a fully formed 2nd order Mandelbrot figure until $a = 6$.

But what gives trigonometric functions such as $[1-\cos(z)]$ and $[z-\sin(z)]$ their 2nd and 3rd order properties respectively, and why are the resulting 6th order Mandelbrots in Figure 31 of different sizes? The rule for predicting fractal order, which we shall justify below, turns out to be surprisingly simple. **Table 1** lists power series expansions for a large number of algebraic functions. ***The fractal order of a given function is the same as the order of the first or lowest term in its power series expansion.*** Indeed, one can designate the first term of the power series expansion of a function as its **reduced function**. At large values of iterations behaves as though the reduced function had been substituted for the given function.

TABLE 1. POWER SERIES EXPRESSIONS FOR VARIOUS FUNCTIONS OF Z

| i.d. | Function | Series Expansion | d |
|--|-----------------|---|----|
| <u>Inverse first order (all expansions begin with z^{-1})</u> | | | |
| -1a. | cosec (z) | $= 1/z + (1/6)z + (7/360)z^3 + (31/15120)z^5 + \dots$ | +1 |
| -1b. | cosech(z) | $= 1/z - (1/6)z + (7/360)z^3 - (31/15120)z^5 + \dots$ | +1 |
| -1c. | cotanh(z) | $= 1/z + (1/3)z - (1/45)z^3 + (2/945)z^5 - \dots$ | +1 |
| -1d. | cotan(z) | $= 1/z - (1/3)z - (1/45)z^3 - (2/945)z^5 - \dots$ | +1 |
| -1e. | arccoth(z) | $= 1/z + 1/3z^3 + 1/5z^5 + 1/7z^7 + \dots$ | +1 |
| <u>Zeroth order (all expansions begin with a numerical constant)</u> | | | |
| 0a. | 1 | $= 1$ | +1 |
| 0b. | e^z | $= 1 + z + z^2/2! + z^3/3! + z^4/4! + z^5/5! + z^6/6! + \dots$ | +1 |
| 0c. | $e^{\tan(z)}$ | $= 1 + z + (1/2!)z^2 + (3/3!)z^3 + (9/4!)z^4 + \dots$ | +1 |
| 0d. | $e^{\sin(z)}$ | $= 1 + z + (1/2!)z^2 - (3/4!)z^4 - (8/5!)z^5 - \dots$ | +1 |
| 0e. | $\sinh(z)/z$ | $= 1 + z^2/3! + z^4/5! + z^6/7! + z^8/9! - \dots$ | +1 |
| 0f. | $\sin(z)/z$ | $= 1 - z^2/3! + z^4/5! - z^6/7! + z^8/9! - \dots$ | +1 |
| 0g. | cosh(z) | $= 1 + z^2/2! + z^4/4! + z^6/6! + z^8/8! - \dots$ | +1 |
| 0h. | cos(z) | $= 1 - z^2/2! + z^4/4! - z^6/6! + z^8/8! - \dots$ | +1 |
| 0i. | sec(z) | $= 1 + z^2/2! + (5/4!)z^4 + (61/6!)z^6 + \dots$ | +1 |
| 0j. | sech(z) | $= 1 - z^2/2! + (5/4!)z^4 - (61/6!)z^6 + \dots$ | +1 |
| 0k. | z^{n-1} | $= -1 + z^n$ | -1 |
| 0l. | $[\sin(z)/z]^n$ | $= -1/3 + (12/5!)z^2 - (30/7!)z^4 + (56/9!)z^6 - \dots$ | -3 |
| <u>First order (all expansions begin with z)</u> | | | |
| 1a. | z | $= +z$ | +1 |
| 1b. | $e^z - 1$ | $= +z + z^2/2! + z^3/3! + z^4/4! + z^5/5! + z^6/6! + \dots$ | +1 |
| 1c. | $\ln(z+1)$ | $= +z - z^2/2 + z^3/3 - z^4/4 + z^5/5 - z^6/6 + \dots$ | +1 |
| 1d. | $\sinh(z)$ | $= +z + z^3/3! + z^5/5! + z^7/7! + z^9/9! + \dots$ | +1 |
| 1e. | $\sin(z)$ | $= +z - z^3/3! + z^5/5! - z^7/7! + z^9/9! + \dots$ | +1 |
| 1f. | arcsin(z) | $= +z + (1/2*3)z^3 + (1*3/2*4*5)z^5 + (1*3*5/2*4*6*7)z^7 + \dots$ | +1 |
| 1g. | arcsinh(z) | $= +z - (1/2*3)z^3 + (1*3/2*4*5)z^5 - (1*3*5/2*4*6*7)z^7 + \dots$ | +1 |
| 1h. | $\tan(z)$ | $= +z + z^3/3 + (2/15)z^5 + (17/315)z^7 + \dots$ | +1 |
| 1i. | $\tanh(z)$ | $= +z - z^3/3 + (2/15)z^5 - (17/315)z^7 + \dots$ | +1 |
| 1j. | arctanh(z) | $= +z + z^3/3 + z^5/5 + z^7/7 + z^9/9 + \dots$ | +1 |
| 1k. | arctan(z) | $= +z - z^3/3 + z^5/5 - z^7/7 + z^9/9 - \dots$ | +1 |

TABLE 1. POWER SERIES EXPRESSIONS FOR VARIOUS FUNCTIONS OF Z (cont'd)

| i.d. | Function | Series Expansion | d |
|--|-------------------------------------|---|-----|
| 1l. | $\sin(z^{3/2})/z^{1/2}$ | $= +z - z^4/3! + z^7/5! - z^{10}/7! + \dots$ | +1 |
| 1m. | $z/(1+z)$ | $= +z - z^2 + z^3 - z^4 + z^5 - z^6 + \dots$ | +1 |
| 1n. | $z/(1+z^2)$ | $= +z - z^3 + z^5 - z^7 + \dots$ | +1 |
| 1o. | $[1-\cos(z)]/z$ | $= +z/2! - z^3/4! + z^5/6! - z^7/8! + \dots$ | +2 |
| 1p. | $[\sin(z)/z]'$ | $= -2z/3! + 4z^3/5! - 6z^5/7! + \dots$ | -3 |
| <u>Second order (all expansions begin with z^2)</u> | | | |
| 2a. | z^2 | $= z^2$ | +1 |
| 2b. | $1-\cos(z)$ | $= +z^2/2! - z^4/4! + z^6/6! - z^8/8! + \dots$ | +2 |
| 2c. | $[z-\sin(z)]/z$ | $= +z^2/3! - z^4/5! + z^6/7! - z^8/9! + \dots$ | +6 |
| 2d. | $\ln[\cos(z)]$ | $= -z^2/2 - z^4/12 - z^6/45 - (17/2520)z^8 - \dots$ | -2 |
| 2e. | $[z-\tan(z)]/z$ | $= -z^2/3 - (2/15)z^4 - (17/315)z^6 - \dots$ | -3 |
| <u>Third order (all expansions begin with z^3)</u> | | | |
| 3a. | z^3 | $= z^3$ | +1 |
| 3b. | $z-\sin(z)$ | $= +z^3/3! - z^5/5! + z^7/7! - z^9/9! + \dots$ | +6 |
| 3c. | $z-\tan(z)$ | $= -z^3/3 - (2/15)z^5 - (17/315)z^7 - \dots$ | -3 |
| <u>Fourth order (all expansions begin with z^4)</u> | | | |
| 4a. | z^4 | $= z^4$ | +1 |
| 4b. | $\sec(z)-\cosh(z)$ | $= (1/6)z^4 + (1/12)z^6 + \dots$ | +6 |
| 4c. | $\operatorname{sech}(z)-\cos(z)$ | $= (1/6)z^4 - (1/12)z^6 + \dots$ | +6 |
| 4d. | $[1-\cos(z)]+\ln[\cos(z)]$ | $= -(1/8)z^4 - (1/48)z^6 - (273/40320)z^8 - \dots$ | -8 |
| <u>Fifth order (all expansions begin with z^5)</u> | | | |
| 5a. | z^5 | $= z^5$ | +1 |
| 5b. | $\arcsin(z)-\sinh(z)$ | $= (1/15)z^5 + (2/45)z^7 + \dots$ | +15 |
| 5c. | $\operatorname{arcsinh}(z)-\sin(z)$ | $= (1/15)z^5 - (2/45)z^7 + \dots$ | +15 |
| 5d. | $\operatorname{arctanh}(z)-\tan(z)$ | $= (1/15)z^5 + (4/45)z^7 + \dots$ | +15 |
| 5e. | $\operatorname{arctan}(z)-\tanh(z)$ | $= (1/15)z^5 - (4/45)z^7 + \dots$ | +15 |

Coefficient d is the divisor of the lowest order term in the series expansion.

As **Figure 32** and Table 1 show, the reduced function for $[1-\cos(z)]$ is $+z^2/2!$, and that for $[z-\sin(z)]$ is $+z^3/3! = z^3/6$. Hence the two functions behave like z^2 and z^3 respectively, and it is reasonable that all four examples in Figure 31 should be 6th order figures.

$[1 - \cos(z)]$ behaves like z^2 ; $[z - \sin(z)]$ like z^3 ? Why?

Series expansion of trigonometric functions: The 1st Term Rule

$\cos(z) = 1 - z^2/2! + z^4/4! - z^6/6! + \dots$

$\underline{1 - \cos(z) = + z^2/2! - z^4/4! + z^6/6! - \dots}$ $n = 2, d = +2! = 2$

$\sin(z) = + z - z^3/3! + z^5/5! - z^7/7! + \dots$

$\underline{z - \sin(z) = + z^3/3! - z^5/5! + z^7/7! + \dots}$ $n = 3, d = +3! = 6$

| Function iterated | Order, n | Factor d in: $a*W_a^5 = d *K$ |
|---------------------|-----------|--------------------------------|
| z^6 | 6 | 1 |
| $z^4*[1 - \cos(z)]$ | $4+2 = 6$ | $1*2 = +2$ |
| $z^3*[z - \sin(z)]$ | $3+3 = 6$ | $1*6 = +6$ |
| $[z - \sin(z)]^2$ | $3+3 = 6$ | $6*6 = +36$ |

32

The other issue in Figure 31 is that of scale or image size. The power series first-term principle again provides the answer. If one iterates z^n/d instead of z^n :

$$z' = a*z^n/d + c \tag{10}$$

this is equivalent to choosing an a value smaller by a factor of d , or $a' = a/d$. The scale product equation then will be:

$$a'*W_a^{n-1} = (a/d)*W_a^{n-1} = K \quad \text{or} \quad a*W_a^{n-1} = |d|*K \tag{11}$$

where as before, W_a is the width of the image measured in some arbitrary but uniform manner. The scale product $a*W_a^{n-1}$ will be larger than its value with z^n by a factor of the magnitude of d .

In sum, the quantity $K = a*W_a^{n-1}/|d|$ is invariant for all functions that yield the same order Mandelbrot figure. If d is negative, it effectively reverses

the sign of a , resulting in the symmetry-reversed Mandelbrot associated with negative a values in Figures 23–24.

Table 2 shows the experimental change in size of mature Mandelbrot figures as measured at $a = 10, 100$ and 1000 , for various combinations of functions that yield 2nd, 3rd and 4th order overall. For the first three examples of 2nd order the scale product $a^*W_a^{n-1}$ is predictably constant and has a value of 3.00 within experimental errors of measurement of image size. In the three subsequent cases the scale products $a^*W_a^{n-1}$ remain constant while a is varied within a given function, but have values which are roughly 2, 3 and 6 times that observed for z^2 .

Replacing each 2nd order function in Table 2 by its reduced function, or the first term of its power series from Table 1, leads to:

| Function | Reduced function | | |
|----------------------------------|--|---------|----------|
| (1) z^*z | $\rightarrow z^2$ | $n = 2$ | $d = +1$ |
| (2) $(e^z-1)*\ln(z+1)$ | $\rightarrow z^*z = z^2$ | $n = 2$ | $d = +1$ |
| (3) $\text{cosec}(z)*z^3$ | $\rightarrow (1/z)*z^3 = z^2$ | $n = 2$ | $d = +1$ |
| (4) $[1-\cos(z)]*1$ | $\rightarrow (z^2/2)*1 = z^2/2$ | $n = 2$ | $d = +2$ |
| (5) $\sin(z)*[\sin(z)/z]'$ | $\rightarrow z^*(-z/3) = -z^2/3$ | $n = 2$ | $d = -3$ |
| (6) $[\sin(z)/z]''*\ln[\cos(z)]$ | $\rightarrow (-1/3)*(-z^2/2) = +z^2/6$ | $n = 2$ | $d = +6$ |

The overall order n is the sum of the orders of the individual functions, while the overall d value is the product of individual d values. The complete scale product Equation 11 predicts that the scale product $a^*W_a^{n-1}$ should be twice as large for case 4 above, three times as large for case 5, and six times as large for case 6, exactly as observed. Furthermore, in case 5 the 2nd order Mandelbrot should be reversed left for right as its negative sign dictates.

The second half of Table 2 tests the scale product equation for 3rd and 4th order iterations. For the first two 3rd order cases, $K = a^*W_a^{n-1}/|d|$ is invariant and equal to ~ 11.5 . For the third example with $d = +6$, however, K at $a = 10$ is only 8.76, and does not rise to the expected ~ 11.5 until a is increased from 10 to 100 to 1000. Similar behavior is seen with the 4th order. The first two examples, with $d = +1$, yield a uniform $K = a^*W_a^{n-1}/|d| = \sim 24.3$. But the last example, with $d = -18$, does not produce this expected K value until a is increased to 1000.

In short, one can determine in advance how a mathematical function will behave upon iteration in Equation 8, by expressing it as a power series and replacing the function by the lowest-order term of the series, or its reduced function. But this reduced function substitution holds only in the limit of large a values, with the threshold of "large enough" varying from one function to another.

TABLE 2. MEASURED SIZE RELATIONSHIPS FOR 2ND, 3RD & 4TH ORDER

| Function | MANDELBROT FIGURES (ER = 10) | | | $(a*W_a^{n-1})$ | | |
|------------------------------|------------------------------|----|------|-----------------|---------------|--------------|
| | n | d | a | W_a | $a*W_a^{n-1}$ | d |
| SECOND ORDER: | | | | | | |
| $z*z = z^2$ | 2 | +1 | 10 | 0.3013 | 3.013 | 3.013 |
| | | | 100 | 0.03001 | 3.001 | 3.001 |
| | | | 1000 | 0.003007 | 3.007 | 3.007 |
| $(e^z-1)*\ln(z+1)$ | 2 | +1 | 10 | 0.3000 | 3.000 | 3.000 |
| | | | 100 | 0.02982 | 2.982 | 2.982 |
| | | | 1000 | 0.003013 | 3.013 | 3.013 |
| $\text{cosec}(z)*z^3$ | 2 | +1 | 10 | 0.3003 | 3.003 | 3.003 |
| | | | 100 | 0.02994 | 2.994 | 2.994 |
| | | | 1000 | 0.002993 | 2.993 | 2.993 |
| $1*[1-\cos(z)]$ | 2 | +2 | 10 | 0.5989 | 5.989 | 2.994 |
| | | | 100 | 0.05995 | 5.995 | 2.998 |
| | | | 1000 | 0.006002 | 6.002 | 3.001 |
| $\sin(z)*[\sin(z)/z]'$ | 2 | -3 | 10 | 0.8891 | 8.891 | 2.964 |
| | | | 100 | 0.09047 | 9.047 | 3.016 |
| | | | 1000 | 0.008982 | 8.982 | 2.994 |
| $[\sin(z)/z]''*\ln[\cos(z)]$ | 2 | +6 | 10 | 1.7887 | 17.89 | 2.981 |
| | | | 100 | 0.1798 | 17.98 | 2.997 |
| | | | 1000 | 0.01804 | 18.04 | 3.007 |
| THIRD ORDER: | | | | | | |
| z^3*1 | 3 | +1 | 10 | 1.070 | 11.45 | 11.45 |
| | | | 100 | 0.3372 | 11.37 | 11.37 |
| | | | 1000 | 0.1066 | 11.36 | 11.36 |
| $z^2*[e^z-1]$ | 3 | +1 | 10 | 1.081 | 10.36 | 10.36 |
| | | | 100 | 0.3403 | 11.58 | 11.58 |
| | | | 1000 | 0.1069 | 11.43 | 11.43 |
| $[z-\sin(z)]*\cos(z)$ | 3 | +6 | 10 | 2.293 | 52.58 | 8.76 |
| | | | 100 | 0.8102 | 65.64 | 10.94 |
| | | | 1000 | 0.2606 | 67.91 | 11.32 |

||

FOURTH ORDER:

| | | | | | | |
|--------------------------------|---|-----|------|--------|-------|--------------|
| $z^3 * z = z^4$ | 4 | +1 | 10 | 1.344 | 24.28 | 24.28 |
| | | | 100 | 0.6230 | 24.18 | 24.18 |
| | | | 1000 | 0.2897 | 24.31 | 24.31 |
| $\cotan(z) * z^5$ | 4 | +1 | 10 | 1.329 | 23.47 | 23.47 |
| | | | 100 | 0.6230 | 24.18 | 24.18 |
| | | | 1000 | 0.2893 | 24.21 | 24.21 |
| $[\sin(z)/z]' * [z - \sin(z)]$ | 4 | -18 | 10 | 3.375 | 384.4 | 21.36 |
| | | | 100 | 1.619 | 424.4 | 23.58 |
| | | | 1000 | 0.7578 | 435.2 | 24.17 |

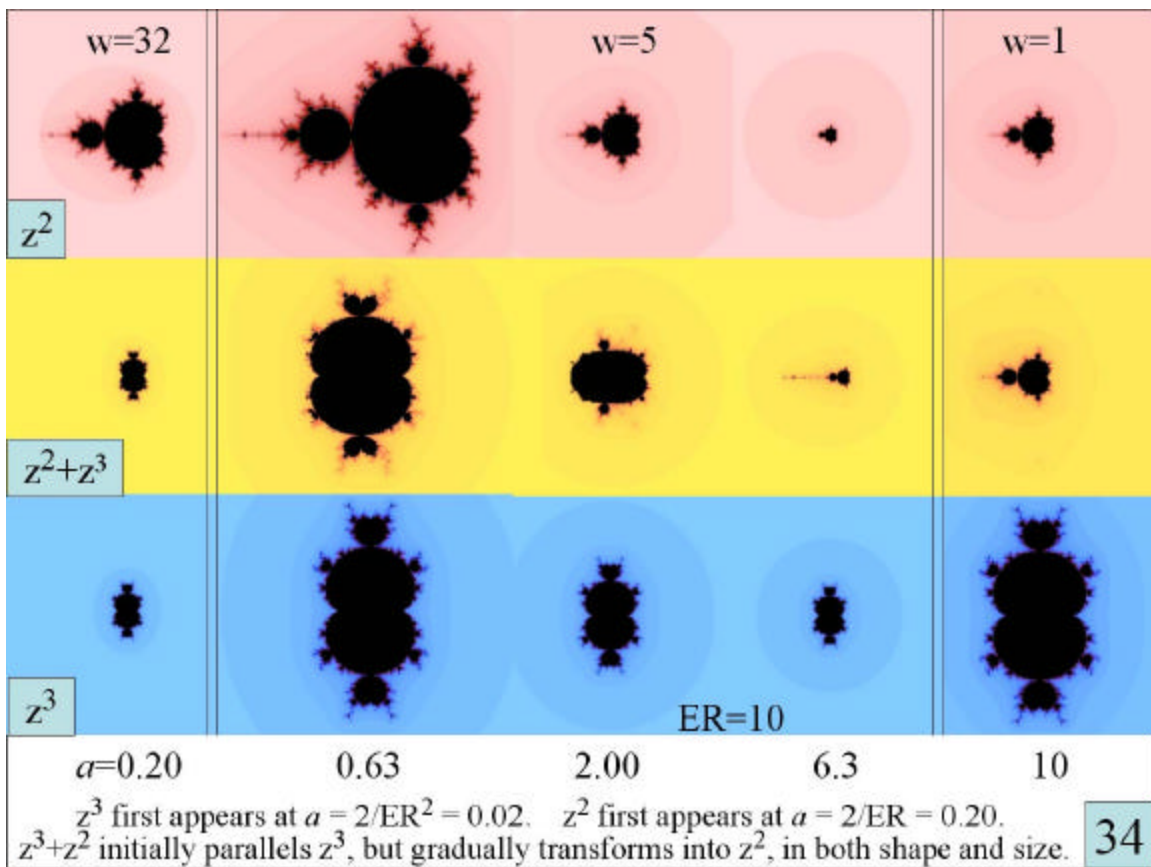
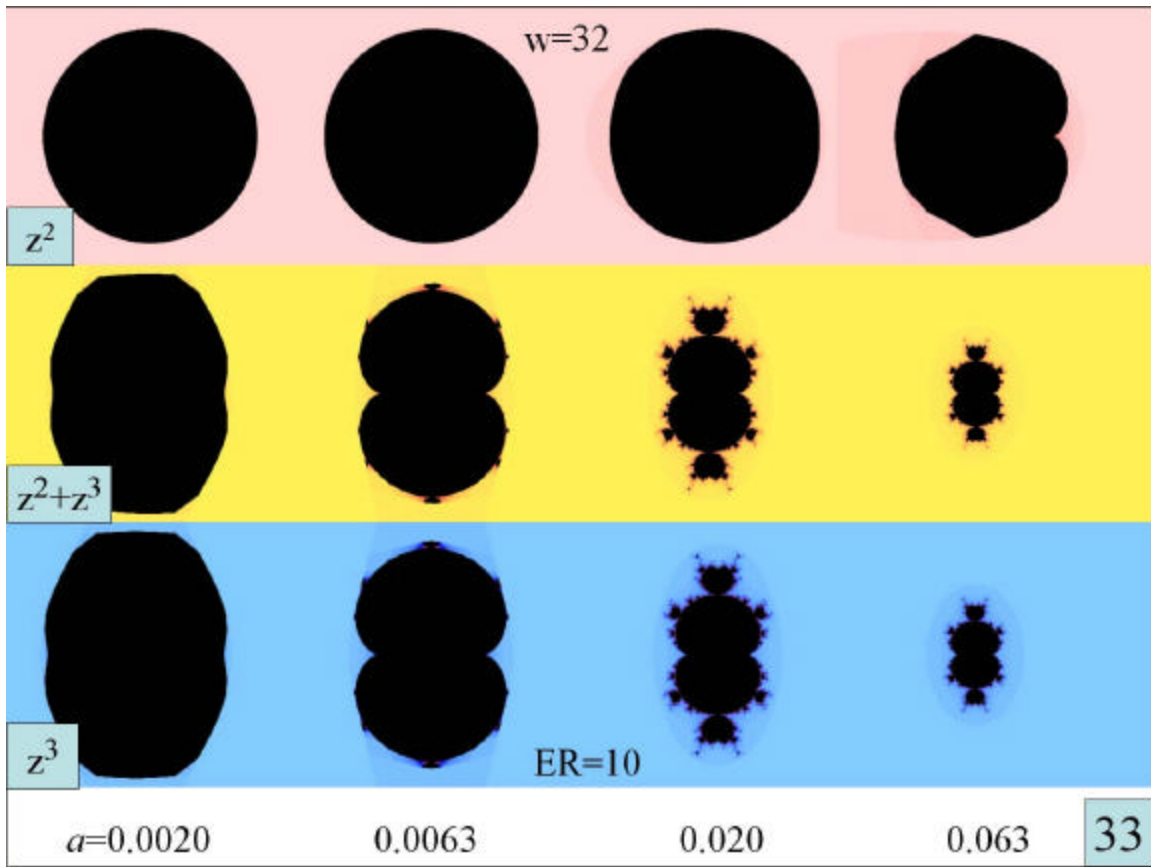
7. Iteration of General Power Series

The preceding section is empirical: it is correct because it works. But why should it work? Why should a mathematical function, at large a , iterate as though it consisted only of the lowest term of its series expansion? To understand this we must have a closer look at power series in general.

(a) $z^3 + z^2$

Figures 33–34 compare iterations of z^2 , $z^3 + z^2$, and z^3 from $a = 0.0020$ through 10, all at $ER=10$. As before, the quantity w is the width of the image frame, not that of the Mandelbrot figure itself. All images shown in Figure 33 are to the same scale, image frame width $w = 32$, as is that in the first column of Figure 34. The next three columns have been enlarged by $32/5$, and the last column by an additional factor of 5. At $a = 0.00063$ (not shown), all three images are perfect disks like that seen for z^2 at $a = 0.002$. As a rises through 0.002 to higher values, z^3 is the first to evolve into a mature Mandelbrot figure, complete by $a = 2/ER^2 = 0.020$, as expected from Equation 7. Iteration of $z^3 + z^2$ produces precisely the same results as z^3 in this range of a . As a continues to rise, z^3 and $z^3 + z^2$ follow the same steady shrinkage calculable from: $a * W_a^2 = \text{constant}$. But between $a = 0.20$ and 0.63 a transformation begins. The $z^3 + z^2$ figure loses its z^3 shape, and evolves into that of z^2 . By ca. $a = 8$ that transformation is complete, and the figure is identical to a z^2 Mandelbrot in both size and shape.

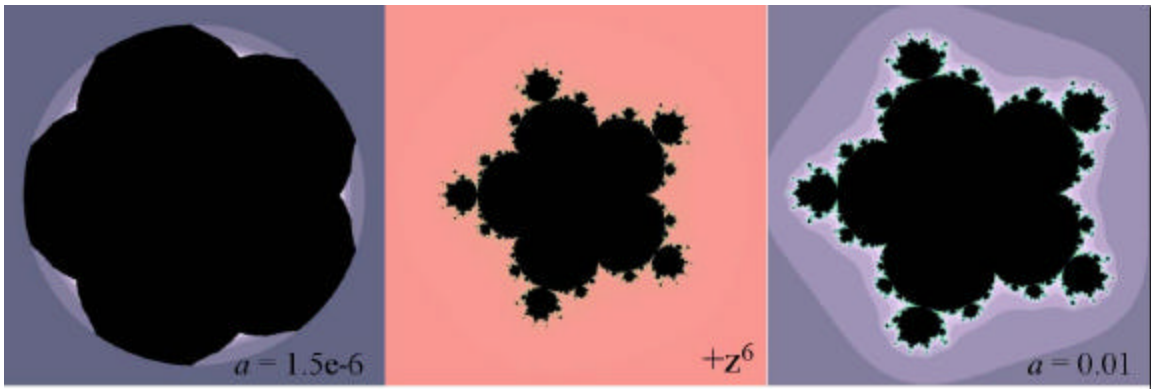
At low values of a , the iterated $z^3 + z^2$ function behaves as though its z^2 term did not exist, and at high value, its z^3 term seemingly does not exist. *The iterated power series is dominated by its highest term at low a , and its lowest term at high a .*



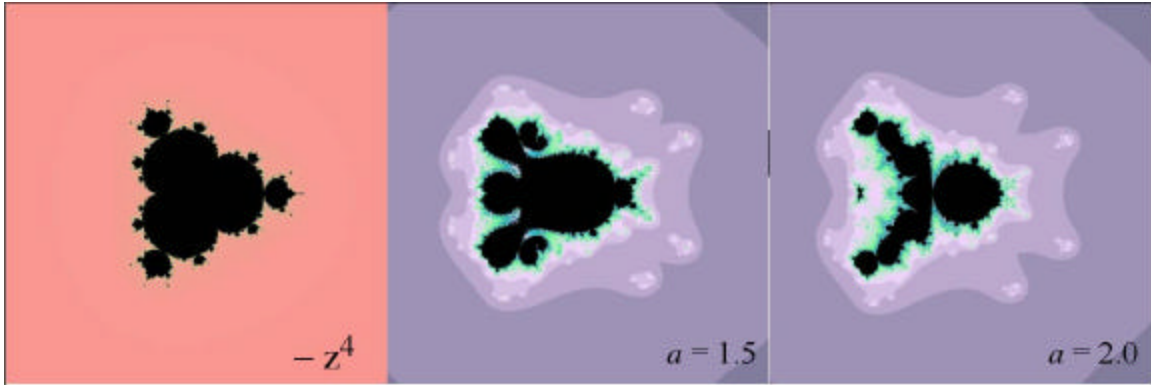
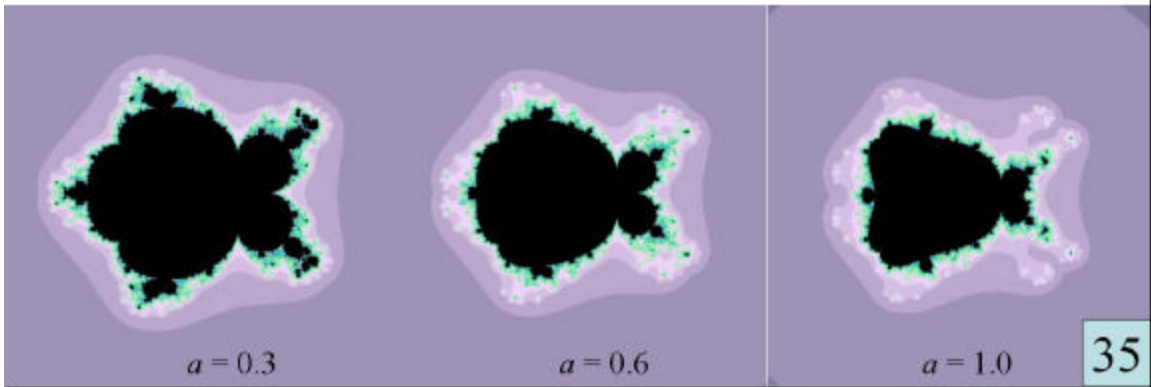
(b) $z^6 - z^4 + z^2$

Figures 35–36 illustrates the way in which each term of a three-term power series can dominate in its own region of a . When the function $F(z) = z^6 - z^4 + z^2$ is iterated with $ER = 10$, a deformed, incomplete pentagonal figure such as that seen here for $a = 1.5 \cdot 10^{-6}$ evolves to completion as a rises to $2.0 \cdot 10^{-5}$, exactly the point expected from $a \cdot ER^5 = 2$ for a simple z^6 Mandelbrot. ($F(z)$ iteration images are in purple, while single-term z^n reference images are in salmon.) The higher power z^6 term continues to dominate until around $a = 0.1$, where deformation begins that will lead to a 2nd order figure at large a . Around 1.0 or 1.5 the figure assumes a roughly triangular shape that is suggestive of a 4th order Mandelbrot, even with its vertex pointing to the right as would be expected for $-z^4$ with a negative value of a .

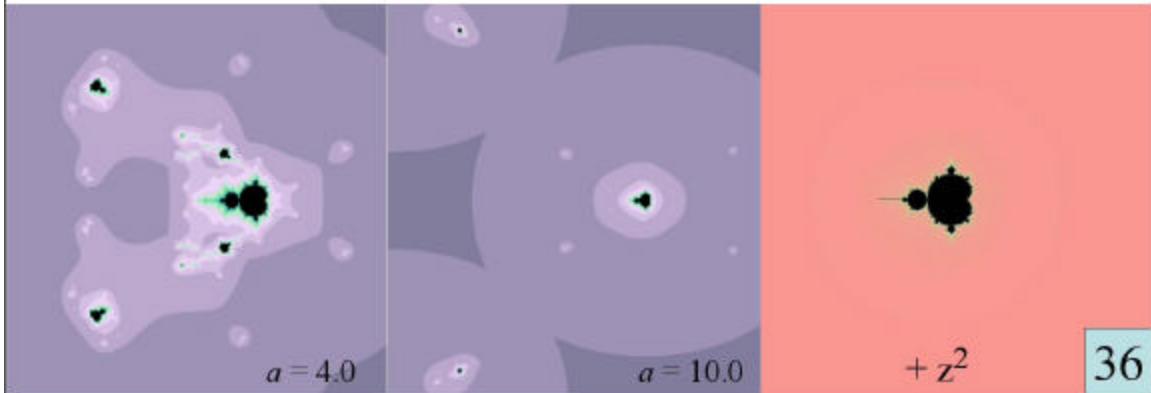
Each of the three terms in the power series seemingly has its own domain of influence: highest term at low a , lowest term at high a , and (more approximately) intermediate term at intermediate a .



Iteration of: $z^6 - z^4 + z^2$. Domains of influence of the 3 terms.



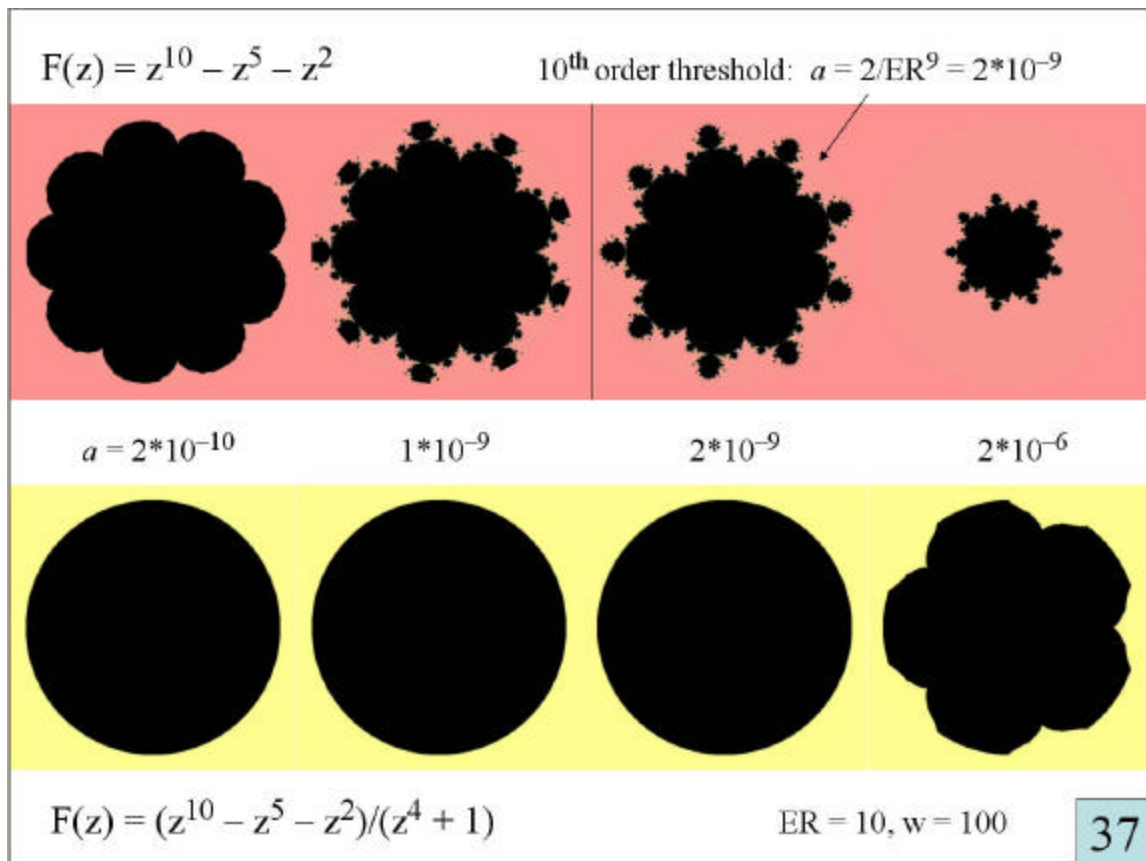
Iteration of: $z^6 - z^4 + z^2$. Domains of influence of the 3 terms.

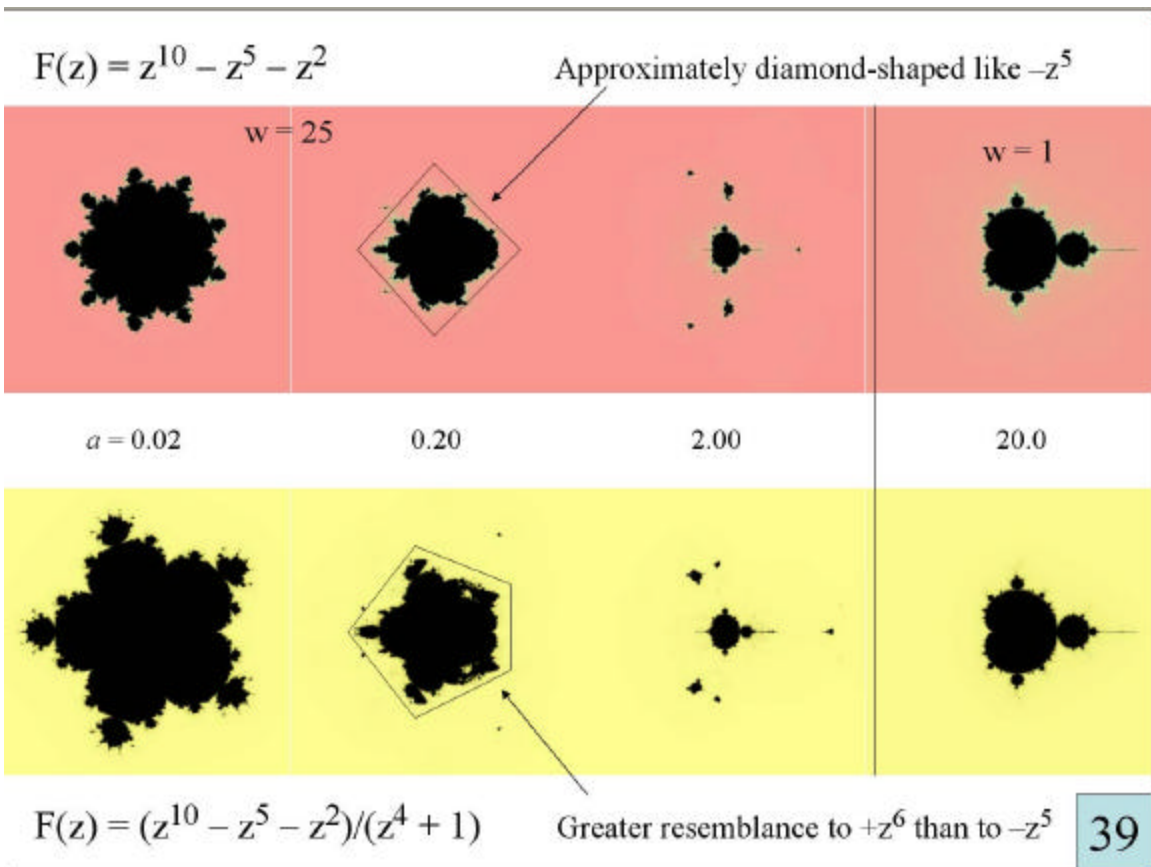
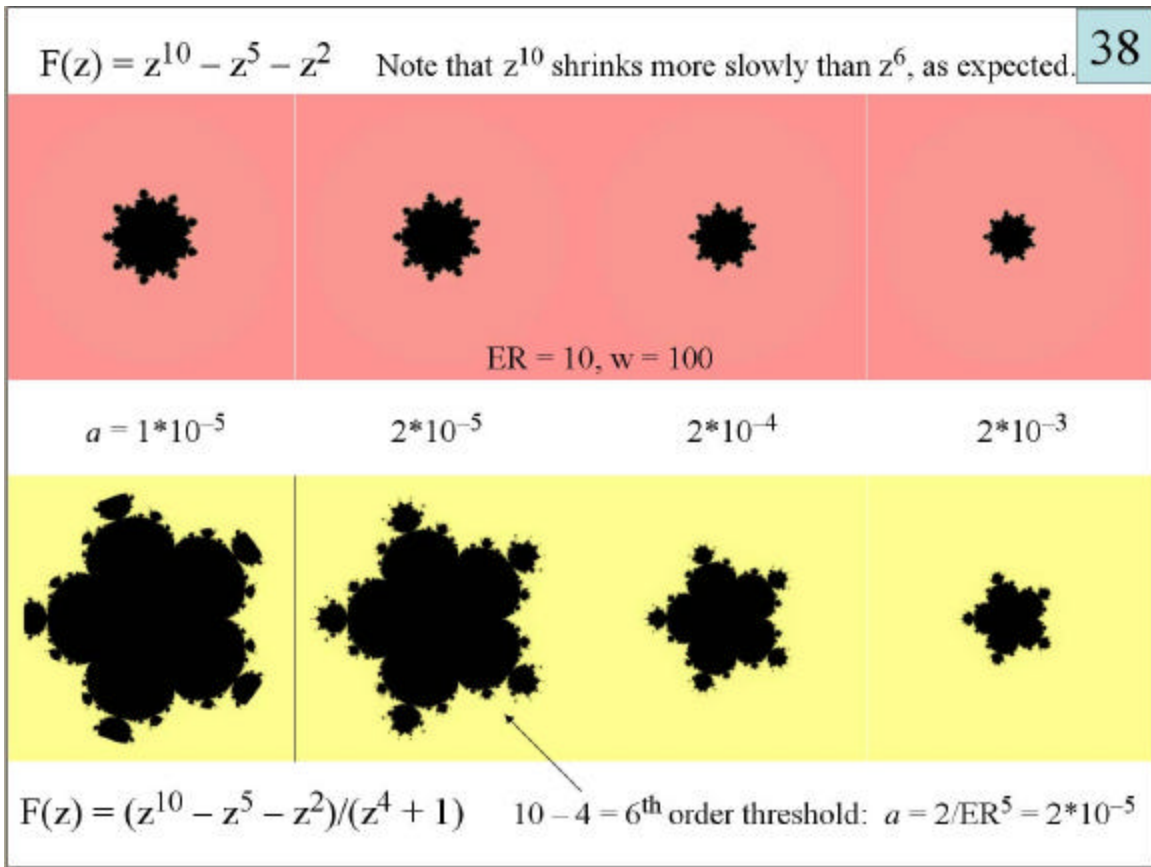


(c) $z^{10}-z^5-z^2$ and $(z^{10}-z^5-z^2)/(z^4+1)$

The iterations of $z^{10}-z^5-z^2$ and $(z^{10}-z^5-z^2)/(z^4+1)$ in **Figures 37-39** again test the idea that, in a three-term power series, the figure produced at intermediate a values bears at least a passing resemblance to that expected from just the middle term of the series, $-z^5$ in this example. They also examine what happens when a is varied during the iteration of the quotient of two power series, $F(z)/G(z)$. These figures display the results of iterating $z^{10}-z^5-z^2$ (top, salmon) and $(z^{10}-z^5-z^2)/(z^4+1)$ (bottom, yellow) at twelve different values of a , generally in tenfold increments, between $2 \cdot 10^{-10}$ and 20.

(1) With $z^{10}-z^5-z^2$, the highest term of the series prevails at low a values (Figure 37). The image is that of a perfect 10th order Mandelbrot. Furthermore, the complete, mature image first occurs at just the a value that would be expected from z^{10} alone: $a = 2/ER^9 = 2 \cdot 10^{-9}$. Below this value the tips of the nine lobes are clipped by the escape radius ($1 \cdot 10^{-9}$), smoothed into hemispheres ($2 \cdot 10^{-10}$), or wiped out entirely on a smooth disk (not shown, but like the $(z^{10}-z^5-z^2)/(z^4+1)$ figure immediately below it).





(2) As expected, the lowest term of the $z^{10}-z^5-z^2$ series prevails at high a (Figure 39). The iterated figure produced is identical in size and shape to that of $-z^2$, reversed left/right as its negative sign requires.

(3) At intermediate a values, $z^{10}-z^5-z^2$ undergoes a transition from the z^{10} figure to that of $-z^2$. The z^{10} image remains up to ca. $a = 0.02$. By $a = 0.20$ (Figure 39) it has assumed approximately the diamond shape expected from the central term of the series, $-z^5$, although this is less definitive than the two extreme images.

(4) At low a values, the highest-power terms of $(z^{10}-z^5-z^2)/(z^4+1)$ predominate *in both numerator and denominator*, as though the function being iterated were: $z^{10}/z^4 = z^6$. The complete, mature 6th order Mandelbrot figure first appears at the a value expected for simple z^6 , or at: $a = 2/ER^5 = 2*10^{-5}$. Below this level the figure is clipped ($1*10^{-5}$), smoothed ($2*10^{-6}$) or totally degraded into a featureless disk ($2*10^{-9}$).

(5) At high a values, $(z^{10}-z^5-z^2)/(z^4+1)$ yields exactly the same reversed $-z^2$ image as does $z^{10}-z^5-z^2$. It behaves as though the lowest power term is dominant *in both numerator and denominator*, or as though the function iterated were: $-z^2/1$.

(6) For $(z^{10}-z^5-z^2)/(z^4+1)$ the intermediate figure at $a = 0.20$ is more ambiguous. It bears a limited resemblance to the $-z^5$ diamond figure from $z^{10}-z^5-z^2$, but also resembles the $+z^6$ figure from which it has evolved.

Note also that Figure 38 illustrates the fact that a 10th order Mandelbrot figure shrinks less rapidly than does a 6th order figure, according to $a*W_a^9 = K$ rather than $a*W_a^5 = K$.

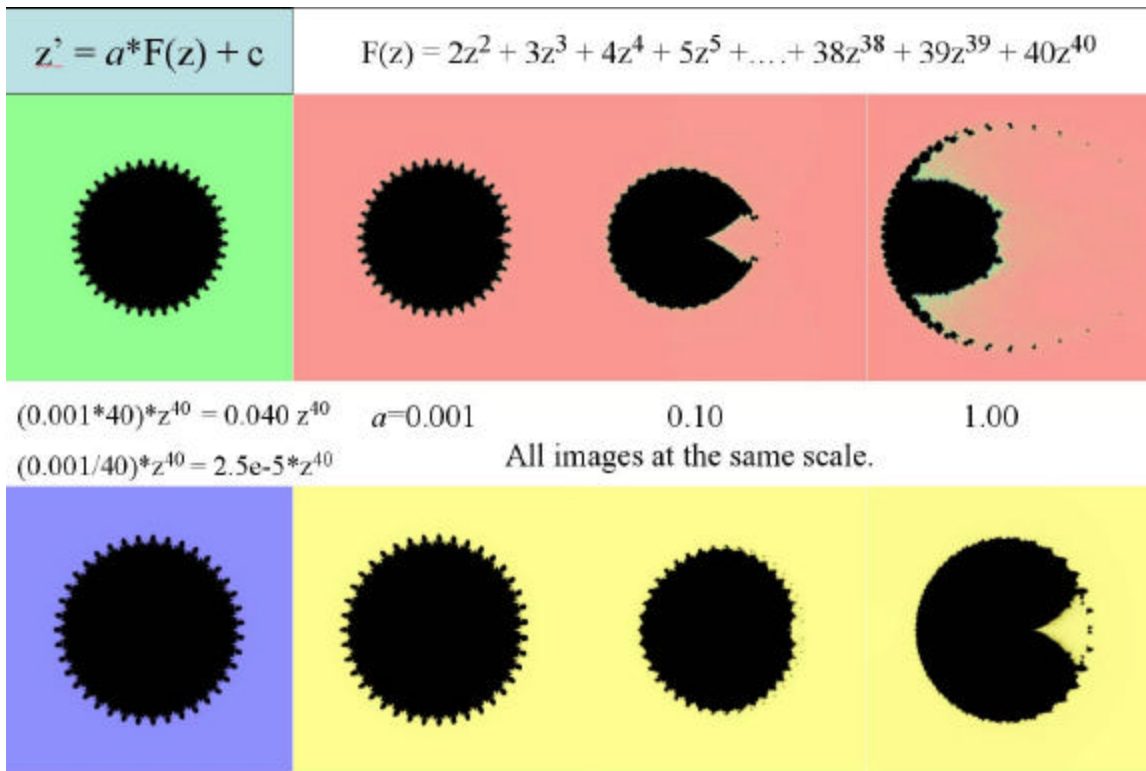
(d) $\sum n*z^n$ and $\sum z^n/n$ with n from 2 to 40

The concept of regions of dominance of highest and lowest power terms is given an especially stringent test in **Figures 40–41**. Two 39–term power series have been constructed, an ascending series (top, salmon):

$$F(z) = 2z^2 + 3z^3 + 4z^4 + 5z^5 + \dots + 38z^{38} + 39z^{39} + 40z^{40}$$

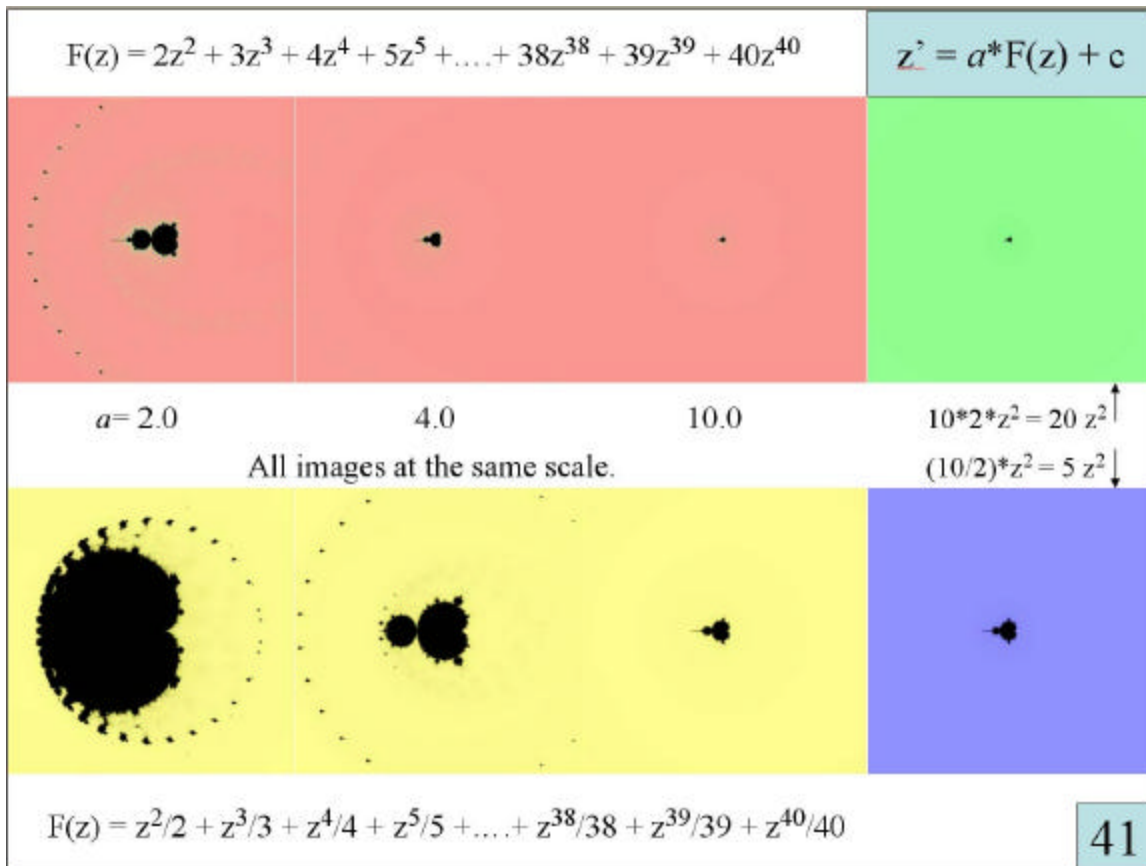
and a descending series (bottom, yellow):

$$F(z) = z^2/2 + z^3/3 + z^4/4 + z^5/5 + \dots + z^{38}/38 + z^{39}/39 + z^{40}/40$$



40

$$F(z) = z^2/2 + z^3/3 + z^4/4 + z^5/5 + \dots + z^{38}/38 + z^{39}/39 + z^{40}/40$$



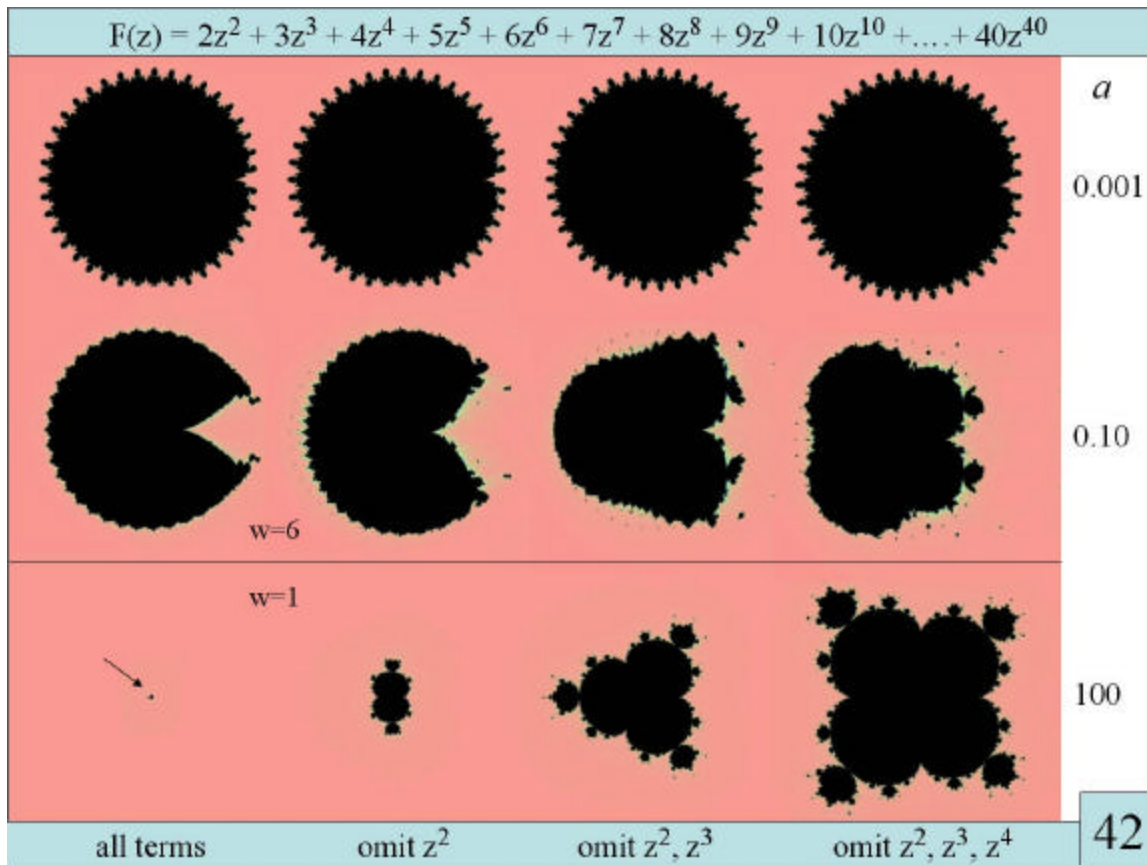
Their iterations are compared with the results of simply iterating z^2 and z^{40} , at equivalent values of a and with the relevant multiplying coefficients of z^2 or z^{40} . The escape radius of $ER=100$ is well above the threshold ER_m in all cases. For both ascending and descending series, the image at $a = 0.001$ (Figure 40) is identical in both size and shape to that which is obtained by iterating $0.001*40*z^{40}$ (top, green) or $0.001*z^{40}/40$ (bottom, violet). At the other extreme, the image at $a = 10$ in Figure 41 is the 2nd order Mandelbrot obtained by iterating $10*2*z^2$ and $10*z^2/2$ for ascending and descending series respectively. But the intermediate transformation steps between the two extremes — 40th order at low a and 2nd order at high a — are quite different in these two test series. The z^{40} disk breaks apart and morphs into a z^2 Mandelbrot more quickly for the ascending series than for the descending. But the end points of the two iterations are the same.

The sizes of the final 2nd order images at $a = 10$ in Figure 41 also obey scale Equation 11. The ascending series has a coefficient of 2, and hence $d = 1/2 = 0.5$. With the descending series, the z^2 coefficient is $1/2$ and $d = 2$. Hence the scale equation for the high- a end of the ascending series is: $a*W_a = 0.5 K$, and that for the descending is: $a*W_a = 2 K$. The measured width of the descending-series image is four times as great as for the ascending series. Identical numbers are obtained when one iterates the relevant single terms in Figure 41, $20*z^2$ for the ascending series (top, green) and $5*z^2$ for the descending (bottom, violet).

Figure 42 shows how sensitive even a long 39-term power series is to the loss of its lowest-order terms. From left to right, iterations are of the complete series, and those with the first, first two, or first three terms deleted. At small a values (top row) the figure is completely independent of the loss of these low order terms; all that matters is the final 40th order term. But at $a = 100$, each figure matches the order of its lowest remaining term, even though these terms had smaller coefficients than any of the other terms:

| Small- a Image | Series Iterated | Large- a Image |
|---------------------|---|---------------------|
| z^{40} | $2z^2+3z^3+4z^4+5z^5+6z^6+7z^7+8z^8+9z^9 + \dots + 39z^{39}+40z^{40}$ | z^2 |
| z^{40} | $3z^3+4z^4+5z^5+6z^6+7z^7+8z^8+9z^9 + \dots + 39z^{39}+40z^{40}$ | z^3 |
| z^{40} | $4z^4+5z^5+6z^6+7z^7+8z^8+9z^9 + \dots + 39z^{39}+40z^{40}$ | z^4 |
| z^{40} | $5z^5+6z^6+7z^7+8z^8+9z^9 + \dots + 39z^{39}+40z^{40}$ | z^5 |

At large a , elimination of low-order terms of the series completely changes the resulting figure, even though the coefficients of the term or terms eliminated are much smaller than those of the remaining terms. But at small a values, the figures for all these series are identical, in this example that of a 40th order Mandelbrot.



8. Application to Infinite Series and Higher Mathematical Functions

In summary, iteration of a power series is a different matter from that of a single exponential term. In the single-term case, constant a has no effect other than determining the size of the resulting figure. *But for a multi-term power series, the shape of the resulting Mandelbrot figure is very much dependent on the particular value of a .* The highest order term in the series dominates at low a , and the lowest order term at high a . In both size and shape of the image, at large a the iterated figure is that which would be obtained if all terms except the lowest-power term did not exist.

This behavior of power series is directly relevant to the issue of why a mathematical function can be replaced by the lowest term of its series expansion at large a . With an infinite series expansion of a mathematical function there is no “highest term”; the series continues without limit. At low a the collection of intermediate power terms yields a complex figure whose structure cannot be predicted easily. But as in all of the examples discussed above, in the limit of high a , only the lowest term of the power series matters; all other terms in the series can be ignored. Hence the validity of the principle defined earlier: **In the limit of large a , a mathematical function can be replaced during iteration by the first or lowest term of its power series expansion, which is defined as its reduced function.**

With this power series background one can understand the reduced-function principle for predicting the results of iteration. All of the 2nd order functions in Table 1 produce a 2nd order Mandelbrot figure when iterated because they commence with a z^2 term. So will two 1st order functions if combined as in Equation 8, because the overall order is the sum of individual orders. A -1st order function such as $\cotan(z)$ iterated with a third order function such as $[z-\tan(z)]$ produces a 2nd order Mandelbrot. Two 2nd order functions iterated together yield a 4th order Mandelbrot. Furthermore, the size of the resultant image depends on the products of the denominators of these lowest-power terms in the manner predicted by the full scale product Equation 11.

To illustrate these principles, consider the combination of $[z-\sin(z)]$ with various other functions in **Figures 43–44**. $[z-\sin(z)]$ is third order, so when it is iterated with -1st, 0th, 1st, 2nd, 3rd, and 4th order functions, the results are the 2nd, 3rd, 4th, 5th, 6th and 7th order Mandelbrot figures shown in Figure 44. Even negative order and zero order functions “follow the rules” of adding exponents.

$$z^{\underline{n}} = a * f(z) * g(z) + c \quad a * W_a^{n-1} = |d| * K$$

$$n = n(f) + n(g) \quad d = d(f) * d(g)$$

$n(f)$ is the order of the lowest term in the series expansion of $f(z)$.

$d(f)$ is the divisor of that same lowest power term.

Reduced functions for the relevant full trigonometric functions:

$$\cot(z) = + z^{-1} - (1/3)z - (1/45)z^3 - \dots \quad n = -1 \quad d = 1$$

$$\cos(z) = 1 - z^2/2! + z^4/4! - z^6/6! + z^8/8! - \dots \quad n = 0 \quad d = 1$$

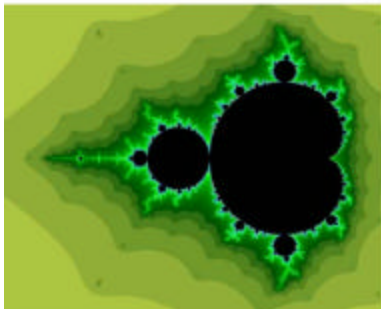
$$\sin(z) = + z - z^3/3! + z^5/5! - z^7/7! + z^9/9! \dots \quad n = 1 \quad d = 1$$

$$1 - \cos(z) = + z^2/2! - z^4/4! + z^6/6! - z^8/8! + \dots \quad n = 2 \quad d = 2$$

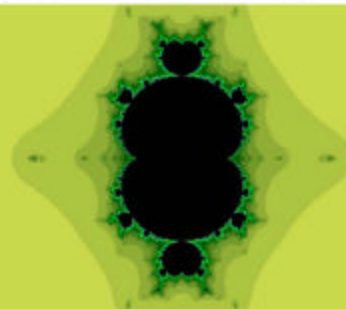
$$z - \sin(z) = + z^3/3! - z^5/5! + z^7/7! - z^9/9! + \dots \quad n = 3 \quad d = 6$$

43

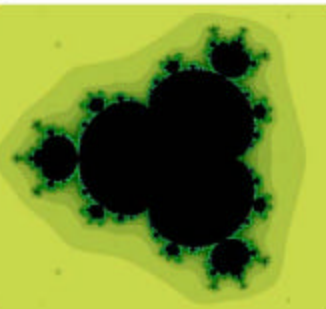
$$z^{\underline{n}} = a * f(z) * g(z) + c \quad n = n(f) + n(g)$$



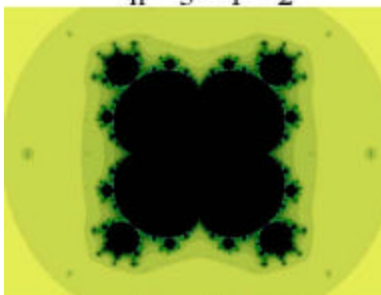
$$[z - \sin(z)] * \cot(z) \\ n = 3 - 1 = 2$$



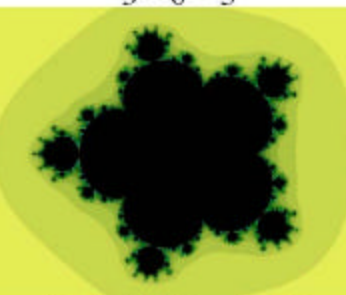
$$[z - \sin(z)] * \cos(z) \\ 3 - 0 = 3$$



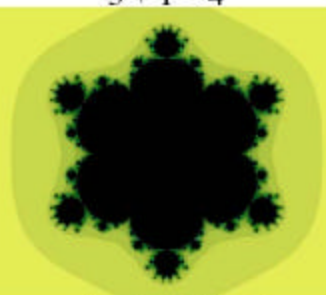
$$[z - \sin(z)] * \sin(z) \\ 3 + 1 = 4$$



$$[z - \sin(z)] * [1 - \cos(z)] \\ n = 3 + 2 = 5$$



$$[z - \sin(z)] * [z - \sin(z)] \\ 3 + 3 = 6$$



$$[z - \sin(z)] * z^4 \\ 3 + 4 = 7$$

44

9. Synthesis of Higher Order Functions by Combining Power Series

Functions whose power series expansions are available in standard reference works are seldom greater than 2nd order. But higher order compound functions can be generated artificially by subtracting pairs of functions whose power series have an identical initial term or terms. 1st order functions 1b through 1n in Table 1 can all be converted to 3rd order functions by subtracting z, thus eliminating the first term of the series as given. The series expansion for [1-cos(z)]/z was synthesized by subtracting the cos(z) series from 1, and then dividing all terms by z.

Sec(z) and cosh(z) have their two first terms in common, so subtracting one from the other as in **Figure 45** creates a 4th order function: sec(z)-cosh(z), whose reduced function is +z⁴/6. Similarly, adding [1-cos(z)] and ln[cos(z)] eliminates their first term and generates another 4th order function, 1-cos(z)+ln[cos(z)], whose reduced function is -z⁴/8. **Table 3** shows that the relative sizes of the three images in Figure 45 is dictated by the scale product equation and the divisors of their reduced functions: d = +1, +6 and -8 respectively. The reversal of the rightmost figure also is consistent with its negative d value.

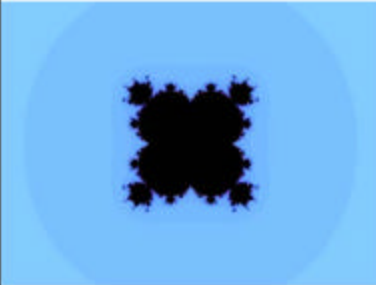
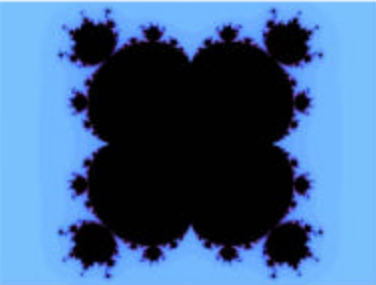
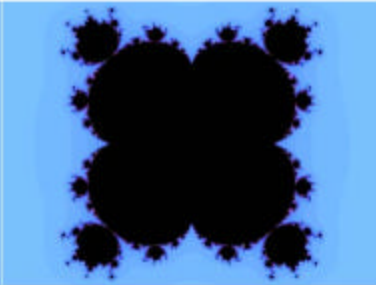
| Fourth power iterations | $z^d = a * F(z) + c$ | $a * W_a^3 = d * K$ |
|---|--|-----------------------------------|
| $sec(z) = 1 + (1/2!)z^2 + (5/4!)z^4 + (61/6!)z^6 + \dots$ | | |
| $cosh(z) = 1 + (1/2!)z^2 + (1/4!)z^4 + (1/6!)z^6 + \dots$ | | |
| $sec(z) - cosh(z) = + (1/6)z^4 + (1/12)z^6 + \dots$ | | |
| | $cos(z) = 1 - (1/2!)z^2 + (1/4!)z^4 - (1/6!)z^6 + \dots$ | |
| | $ln[cos(z)] = - (1/2)z^2 - (1/12)z^4 - (1/45)z^6 - \dots$ | |
| | $1 - cos(z) + ln[cos(z)] = - (1/8)z^4 - (1/48)z^6 - \dots$ | |
| | | |
| $F(z) = z^4$ $d = +1$ | $sec(z) - cosh(z)$ $+6$ | $1 - cos(z) + ln[cos(z)]$ -8 |

TABLE 3. TESTS OF SIZE RELATIONSHIPS IN 4TH AND 5TH ORDER ITERATIONS

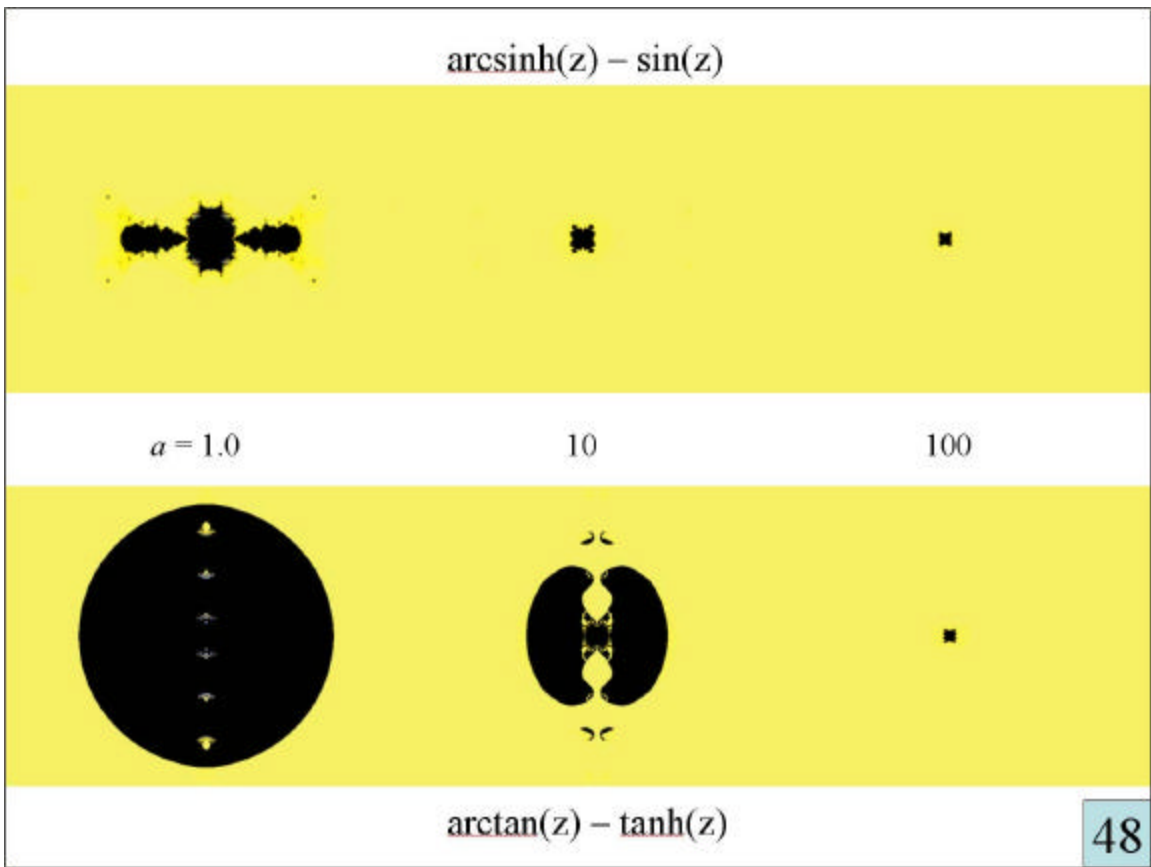
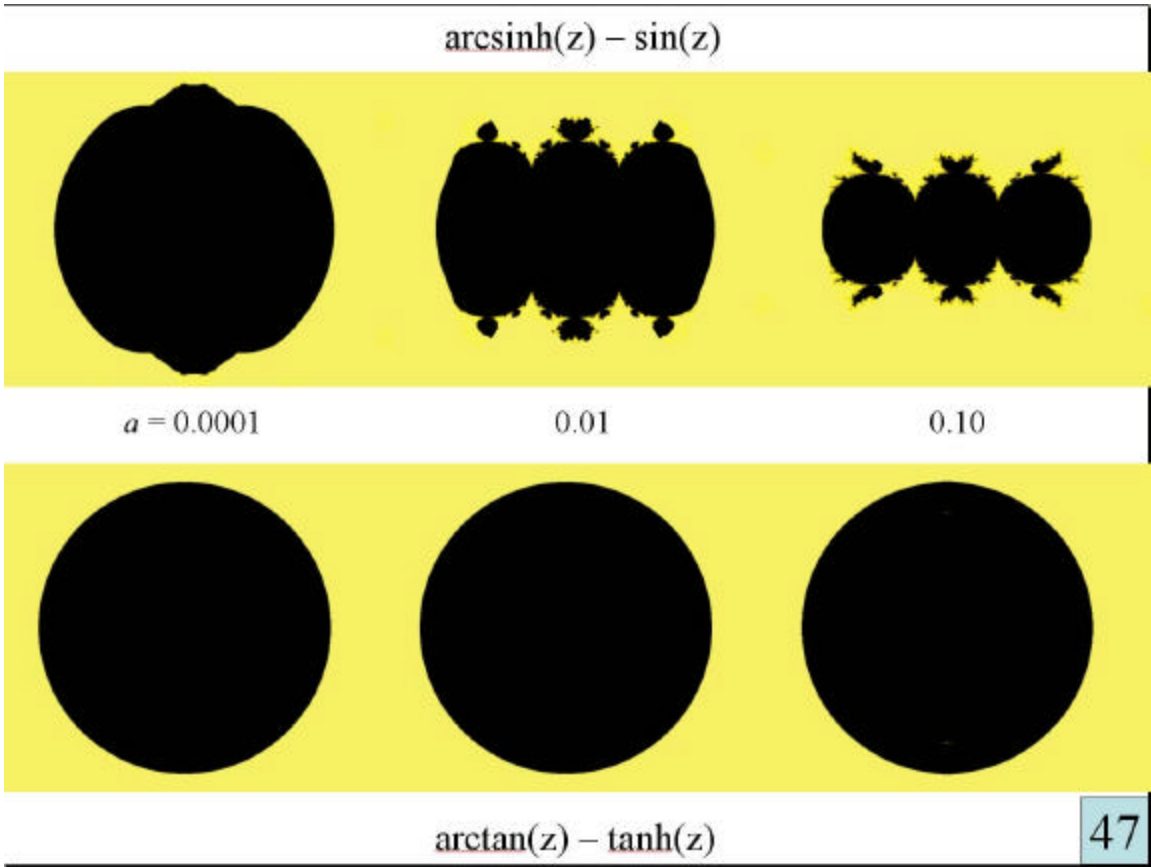
| Function | (ER = 10) | | a | W _a | a*W _a ⁿ⁻¹ | (a*W _a ⁿ⁻¹) |
|-----------------------|-----------|-----|-----------------|----------------|---------------------------------|------------------------------------|
| | n | d | | | | d |
| FOURTH ORDER: | | | | | | |
| z ⁴ | 4 | +1 | 10 ³ | 0.2898 | 24.30 | 24.30 |
| sec(z)-cosh(z) | 4 | +6 | 10 ³ | 0.5267 | 146.1 | 24.35 |
| [1-cos(z)]+ln[cos(z)] | 4 | -8 | 10 ³ | 0.5796 | 194.7 | 24.34 |
| FIFTH ORDER: | | | | | | |
| z ⁵ | 5 | +1 | 10 ³ | 0.4237 | 32.23 | 32.23 |
| arcsinh(z)-sin(z) | 5 | +15 | 10 ³ | 0.8411 | 500.5 | 37.37 |
| arctan(z)-tanh(z) | 5 | +15 | 10 ³ | 0.8460 | 512.2 | 34.15 |
| z ⁵ | 5 | +1 | 10 ⁶ | 0.0754 | 32.32 | 32.32 |
| arcsinh(z)-sin(z) | 5 | +15 | 10 ⁶ | 0.1483 | 483.7 | 32.25 |
| arctan(z)-tanh(z) | 5 | +15 | 10 ⁶ | 0.1485 | 486.3 | 32.42 |

The expected 4th or 5th order images are obtained in all cases above, and that for [1-cos(z)]+ln[cos(z)] is reversed as its negative d value predicts. Note from the bold face figures at lower right that the scale product equation becomes more accurate when a is increased from 10³ to 10⁶.

In a similar manner the four combinations of sine- and tangent-related functions listed as 5b through 5e in Table 1 all have 5th order initial terms, +z⁵/15. Iteration yields ideal 5th order Mandelbrots like that for z⁵ but larger in the way that the scale product equation and their 15-fold larger d values would predict (**Figure 46**). It would be interesting to iterate the quadruple function: arcsinh(z)-sin(z)-arctan(z)+tanh(z), which has a reduced function of +(2/45)z⁷, and hence would yield a 7th order Mandelbrot with scale parameter d = 22.5. Regrettably, this calculation is beyond the abilities of either the *Fractal Explorer* or *Fractal Domains* programs.

| Fifth power iterations | $z^2 = a * F(z) + c$ | $a * W_a^4 = d * K$ |
|---|---|--|
| $\operatorname{arcsinh}(z) = +z - (1/2*3)z^3 + (1*3/2*4*5)z^5 - (1*3*5/2*4*6*7)z^7 + \dots$ | | |
| $\sin(z) = +z - (1/3!)z^3 + (1/5!)z^5 - (1/7!)z^7 + \dots$ | | |
| <hr/> | | |
| $\operatorname{arcsinh}(z) - \sin(z) = + (1/15)z^5 - (2/45)z^7 + \dots$ | | |
| | $\arctan(z) = +z - (1/3)z^3 + (1/5)z^5 - (1/7)z^7 + \dots$ | |
| | $\tanh(z) = +z - (1/3)z^3 + (2/15)z^5 - (17/315)z^7 + \dots$ | |
| | $\arctan(z) - \tanh(z) = + (1/15)z^5 - (4/45)z^7 - \dots$ | |
|  |  |  |
| $F(z) = z^5$ $d = +1$ | $\operatorname{arcsinh}(z) - \sin(z)$ $+15$ | $\arctan(z) - \tanh(z)$ $+15$ |
| | | 46 |

Although $\operatorname{arcsinh}(z) - \sin(z)$ and $\arctan(z) - \tanh(z)$ reach the same limiting figure (Figure 46), their manner of getting there from the initial $a = 0$ parent disk is quite different (**Figures 47–48**). The $\operatorname{arcsinh}(z) - \sin(z)$ parent disk at first collapses onto the horizontal axis. By $a = 3$ a misshapen but recognizable square 5th order Mandelbrot is visible at the origin, and it subsequently regularizes while the remaining fragments decay and vanish. In contrast, the $\arctan(z) - \tanh(z)$ parent disk persists through $a = 1$ and more. Beyond $a = 5$ the disk begins to shrink around the origin, but does not vanish to reveal a tiny central 5th order Mandelbrot until around $a = 23$. Related functions $\operatorname{arcsin}(z) - \sinh(z)$ and $\operatorname{arctanh}(z) - \tan(z)$ are identical to these except for 90° rotation about the origin. These calculations were performed using $ER = 10$. Altering ER produces minor changes as expected from the earlier discussion, but the overall differences in behavior remain.



These results emphasize the principles that (a) replacement of a given function by its reduced function is an approximation that only becomes fully valid in the limit of large a , and (b) the rate and pathway of convergence to this limit are very much a property of the individual function examined. For the 4th order examples of Table 3, the observed $(a^*W_a^{n-1})/|d| = 24.3$ seen with $d = 1$ is satisfactorily duplicated by higher d values at $a = 1000$, whereas for the 5th order functions that we have just been examining, $(a^*W_a^{n-1})/|d|$ is not yet constant at $a = 1000$, and only becomes so two or three orders of magnitude beyond.

10. The Natural History of Mandelbrot Figures

All of the foregoing can be summarized in the following seven principles. With these principles one can understand how iterations behave at higher powers, how they depend on positive and negative scale coefficients a , and why simple power series and various higher mathematical functions iterate to produce the images that are encountered:

I. Iteration of the n^{th} order function $z' = a^*z^n + c$ results in a Mandelbrot figure displaying $n-1$ lobes of density extending outward around its perimeter, separated by $n-1$ deep tapered junctions. For negative values of a , the figure is identical to that for positive values, but rotated in a way that interchanges positions of lobes and junctions.

II. Practical determination of whether a point is to be included or excluded from the Mandelbrot set involves choosing an escape radius, ER. This ER must remain larger than the Mandelbrot image; if not, then the image is truncated and degraded. The minimum escape radius ER_m depends on both order, n , and scale factor, a , according to: $ER_m^{n-1} = 2/a$. If the chosen ER is larger than this minimum value, then it exerts no effect on the Mandelbrot image. A truncated or incomplete Mandelbrot image can be given its mature form by increasing either a or ER or both, to the point where once again, $a^*ER^{n-1} = 2$.

III. As a increases, the Mandelbrot figure shrinks according to the scale product equation: $a^*W_a^{n-1} = K$, where K is a constant for a given order, n , and for a given manner of measuring figure size. Higher order Mandelbrots shrink less rapidly than lower order. For simple z^n Mandelbrots, the choice of a has no effect on the figure produced other than that of size, above the threshold escape radius, ER_m .

IV. If z^n in the iteration equation is replaced by z^n/d , then constant K in the scale product equation is increased by the same factor, or: $a^*W_a^{n-1} = |d| * K$.

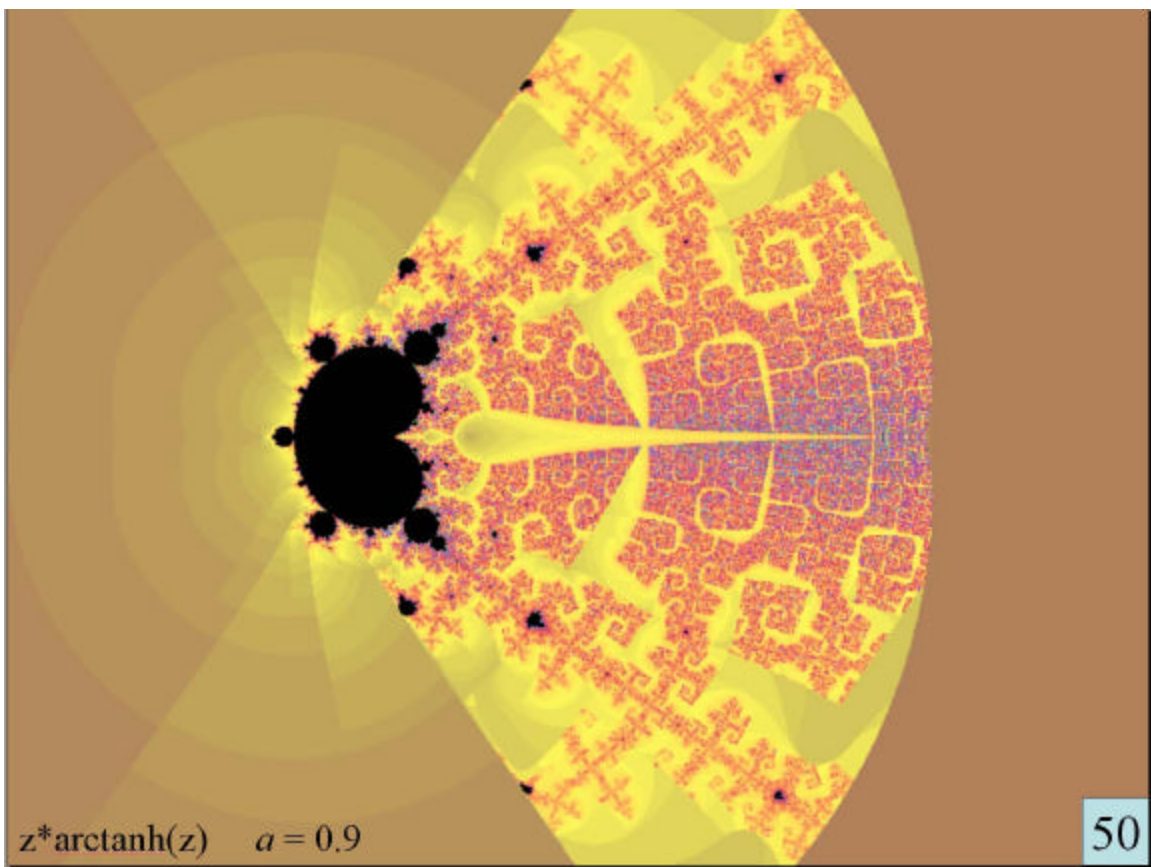
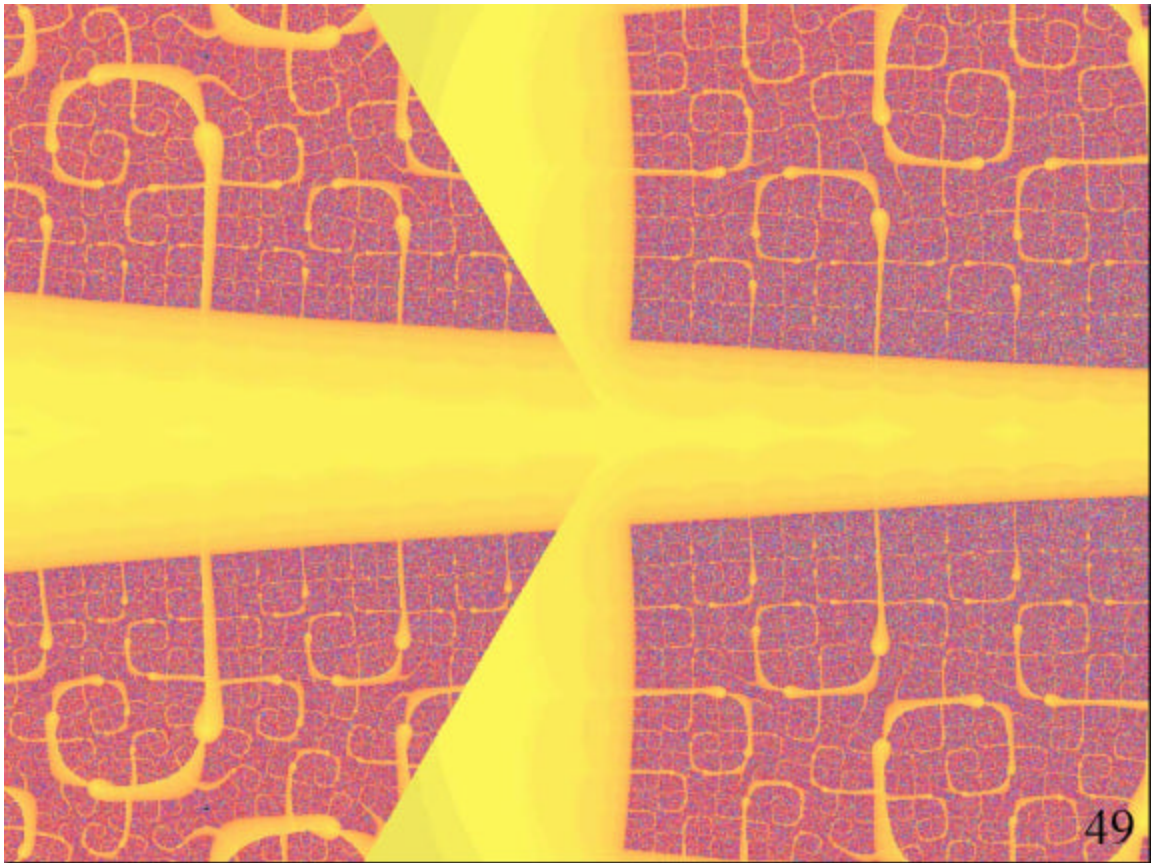
V. When a multi-term power series is iterated, the highest power term dominates at low a values, and the lowest order term takes over completely in

the limit of large a . A mathematical function that can be expressed as an infinite series can be considered as a power series with no maximum term. Only the dominance of the lowest power term at large a remains.

VI. When the iteration equation is generalized to: $z' = a*f(z)*g(z) + c = a*F(z) + c$, each of the functions $f(z)$ and $g(z)$ can be regarded as exhibiting a characteristic order. If their combined order is n , then the ultimate Mandelbrot figure at large values of a or ER will be identical to that produced by iterating a simple z^n , except for scale.

VII. By principle V above, the order of a chosen function $f(z)$ is the order of the lowest term in its power series expansion. In fact, the first term of that series can be designated as the *reduced function*, and where behavior at large a or ER values is concerned, the reduced function can be substituted for the function itself. If $f(z) = [1-\cos(z)] = +z^2/2! - z^4/4! + \dots$ and $g(z) = [z-\tan(z)] = -z^3/3 - (2/15)z^5 + \dots$ then iteration of $[1-\cos(z)]*[z-\tan(z)]$ for large values of a is the same as iterating: $(z^2/2!)*(-z^3/3)$ or $-z^5/6$. The result will be a 5th order Mandelbrot figure, with lobes and junctions interchanged as the minus sign dictates. It will obey a scale product equation of: $a*W_a^4 = 6*K$, where K is the scale product when a simple z^5 is iterated.

The 2nd order Mandelbrot figure of Figure 3 has been an object of intensive study over the past 20 years, with its advocates marveling over the intricacy and beauty of its many levels of detail. Yet each of the higher Mandelbrot figures described in this paper is its equal in complexity, beauty and interest, and just as worthy of careful study. Studying only the z^2 set to the exclusion of all others is as limiting as trying to compose a Bach fugue using only one note. The title page drawing of **Figure 1** shows a small part of the intricacy contained in the iteration of $[z-\sin(z)]*\arctan(z)$ with $a = 1.0$. **Figure 49** might be termed the “national flag of the Republic of Fractovia”, and suggests that Fractovia must be Scandinavian. **Figure 50** shows its source in the iteration of $z*\operatorname{arctanh}(z)$ with $a = 0.90$. The “flag” is found just to the right of a black object that by $a = 2.0$ will have evolved into a mature 2nd order Mandelbrot.

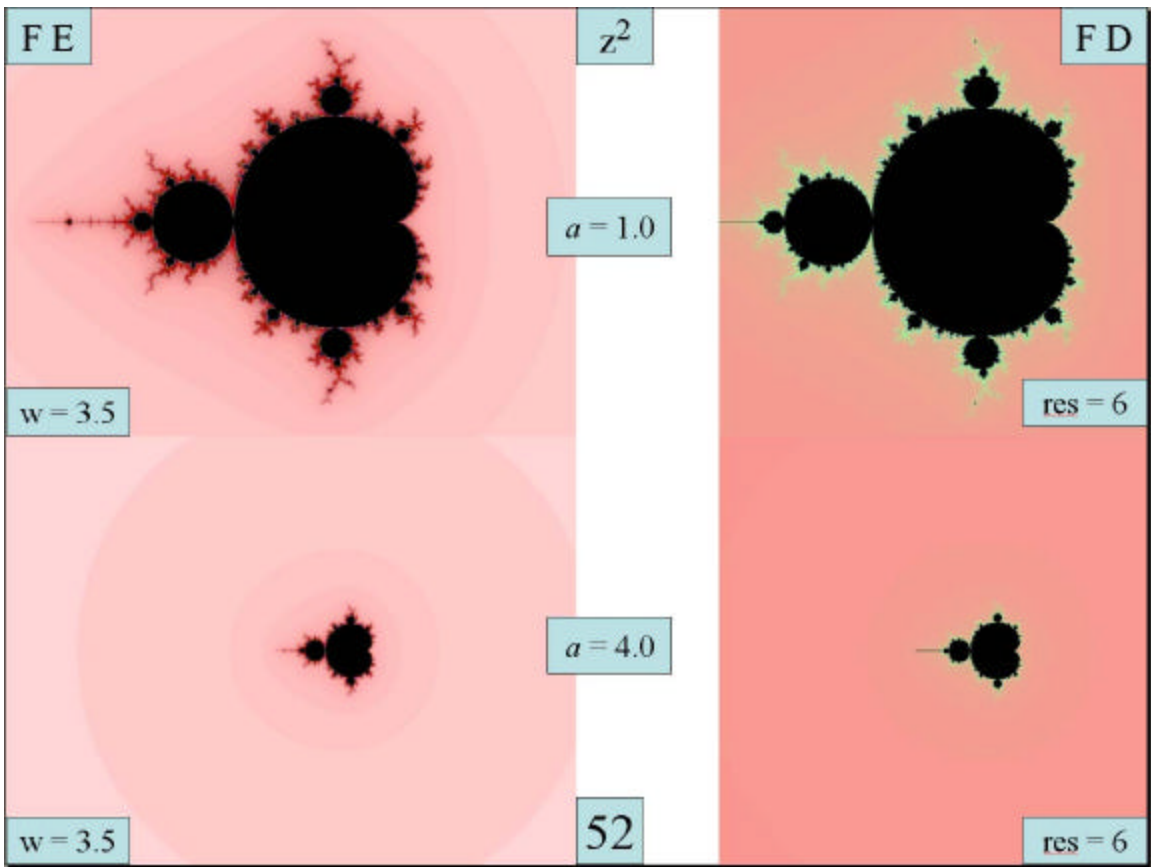
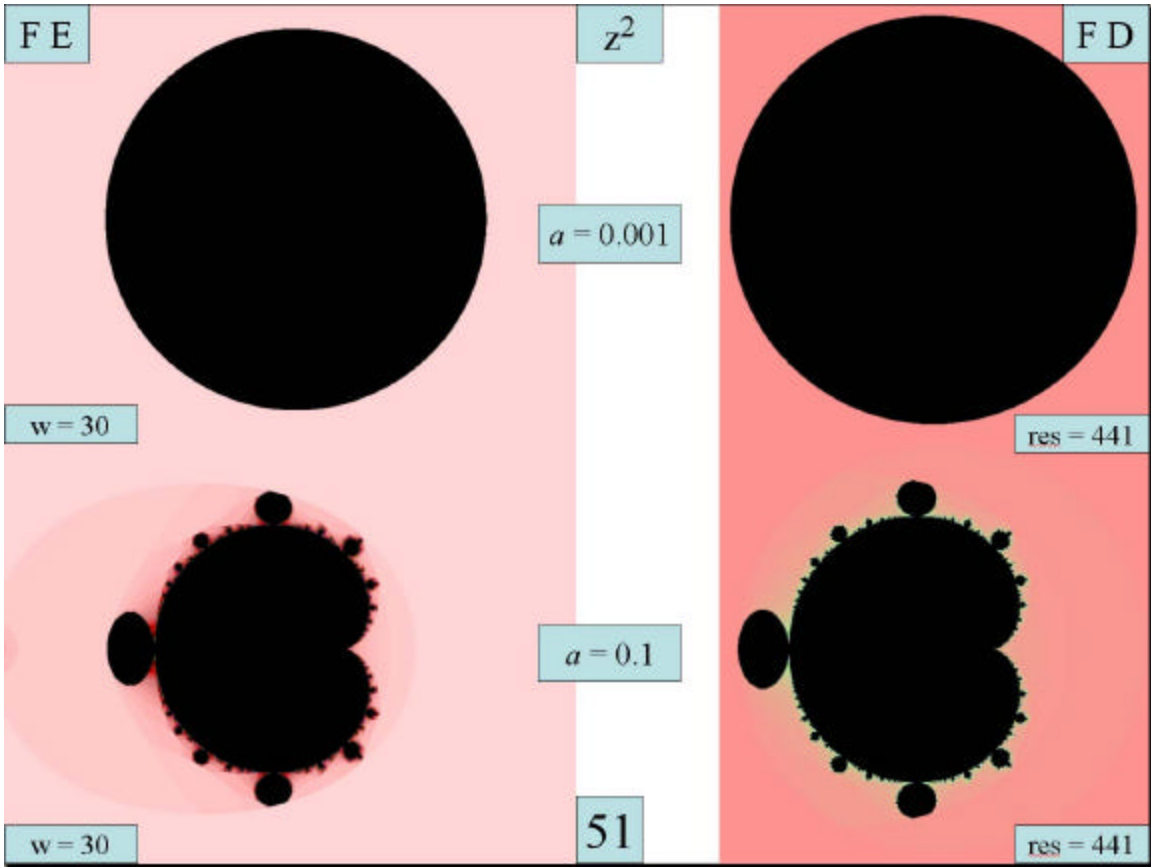


One's first impression of fractal figures is one of enormous complexity, with endless new details no matter how much the figure is magnified. Iterations using various powers of z , or various mathematical functions, appear to be as intricate and confusing as the fractals themselves. But a pleasing regularity emerges, and fractal iteration processes are seen to follow simple and well-defined rules. There is indeed order amidst the chaos, and it is this order that gives fractal geometry its strong attraction.

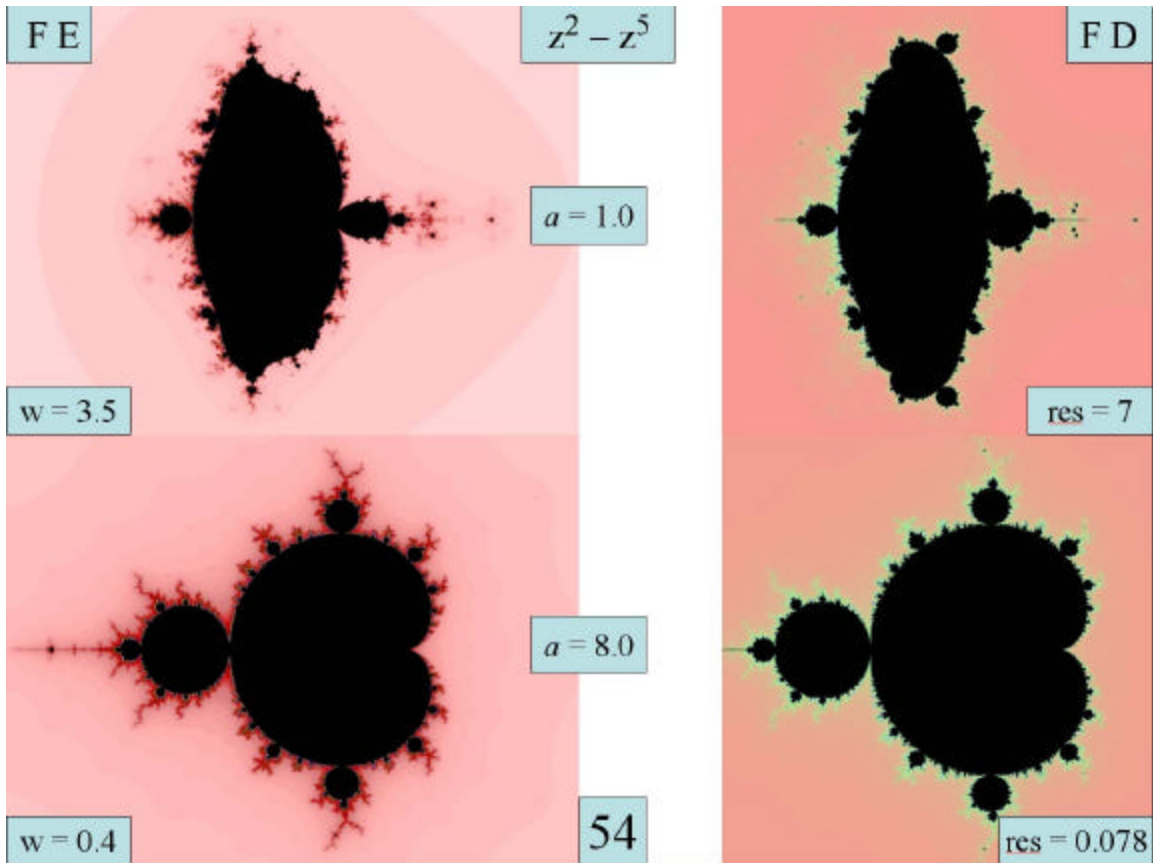
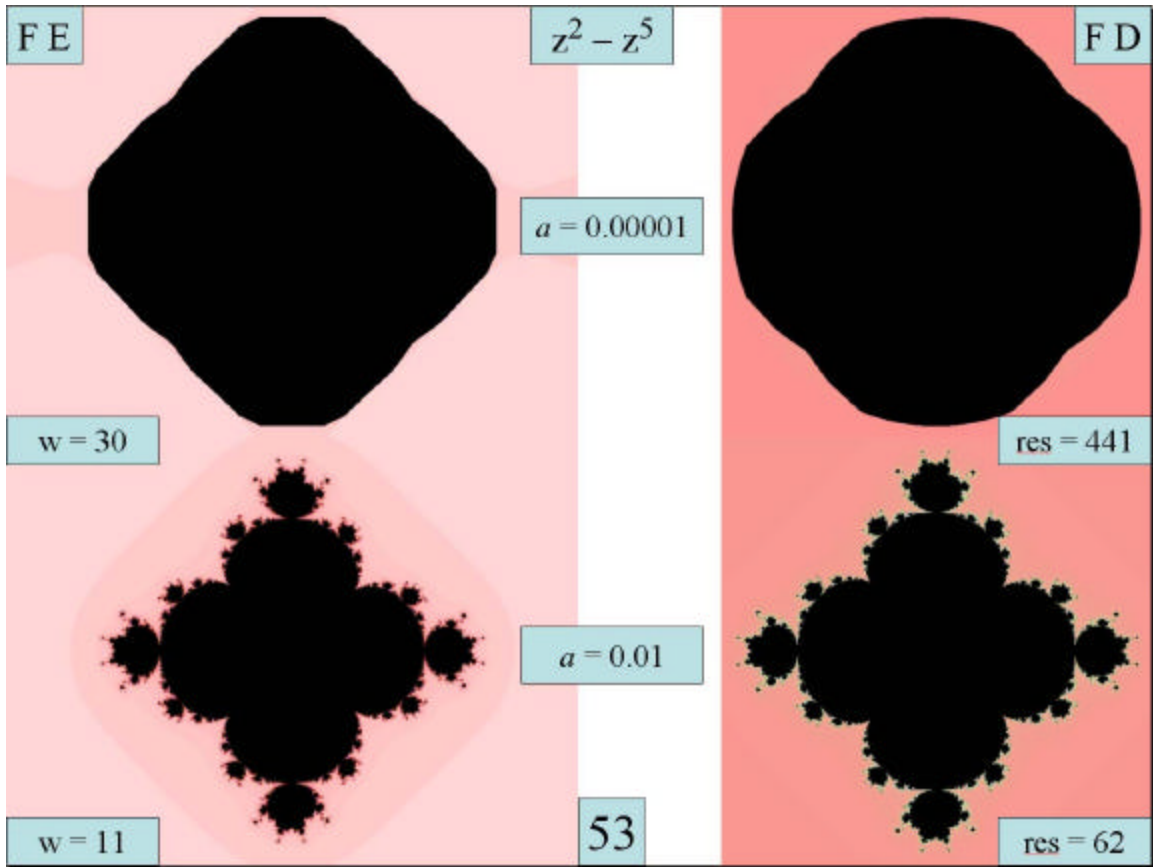
APPENDIX: COMPARISON OF RESULTS WITH TWO DIFFERENT FRACTAL PROGRAMS

This analysis was carried out with the aid of two different but equally useful programs for the Macintosh: *Fractal Domains* by Dennis C. De Mars (demars@kagi.com), and *Fractal Explorer* by Peter Stone (peterstone@optusnet.com.au). FD is shareware, available from <http://www.fractaldomains.com>. FE is freeware, available from <http://members.optusnet.com.au/~peterstone>. FD is especially useful in allowing one to iterate any desired polynomial or quotient of two polynomials. FE, in turn, provides access to a vast array of trigonometric, exponential and logarithmic functions. Both programs have straightforward (although quite different) construction, offer excellent color graphics, and permit searching through fourteen orders of magnification.

These two different but complementary programs offer the opportunity of independent testing of the principal ideas of this paper. **Figures 51–52** compare results with *Fractal Explorer* (left) and *Fractal Domains* (right) of iterating the basic 2nd order equation: $z' = a*z^2 + c$ for various values of a from 0.001 to 4.0. Equivalent parameters have been used in both cases: an escape radius of $ER = 10$ for FD and an escape constant $EC = ER^2 = 100$ for FE. Resolution (res) in FD is a measure of picture area, and is proportional to the square of the picture width (w) employed by FE. Identical magnifications are used in equivalent figures obtained by both programs. In both FE and FD, the 2nd order figure at or near $a = 0$ is a featureless black disk because ER_m is much larger than 10. By $a = 0.1$ this disk has evolved into an incomplete 2nd order Mandelbrot figure, identical in size and shape in the two programs. By $a = 1.0$ the figure has reached its final mature form, and only shrinks in size thereafter according to the scale product Equation 6.



Figures 53–54 offer an even sterner program comparison: iteration of the two-term power function $z' = a*(z^2-z^5) + c$ at various a values. For FD this is accomplished by defining the function in a straightforward manner as: $a*z^2-a*z^5$. With FE the process is a little more involved, requiring iteration of the product of two built-in functions, z^2 and z^3-1 , using negative a values—i.e.: $-a*z^2*(z^3-1) = a*(z^2-z^5)$. But the results with the two programs are identical in size and shape at equivalent a values. At $a = 0.00001$ the image is distorted and smoothed because $ER = 10$ is too small. Around $a = 0.01$ a classic 5th power Mandelbrot figure is encountered, even being rotated 45° from a square to the diamond shape as predicted by the minus sign in $-z^5$. The two programs continue through the same elongated intermediate figure around $a = 1$, as the 5th power Mandelbrot converts into a 2nd power Mandelbrot that is complete around $a = 8.0$. Other conclusions of this paper, where possible, have also been verified using both programs. These two programs, FD and FE, are highly recommended to anyone with even a casual interest in fractal geometry.



ACKNOWLEDGEMENTS

I would like to thank Peter Stone and Dennis De Mars first for writing and making available such useful fractal programs, and then for being willing to discuss them by mail and e-mail with an interested user. I am grateful to Prof. Dr. Dietmar Saupe of the University of Konstanz for comments that cleared up misunderstandings in early drafts of this work. But most of all I appreciate the continued interactions and discussions with Prof. Robert L. Devaney of Boston University. He pointed out weaknesses in some subjects, persuaded me to delete others, and helped me put fractals on a rational basis. While he undoubtedly still would not agree with me about everything in this paper, I have learned much from his guidance.

I am always glad to hear from others interested in fractals, and can be reached at: **red@mbl.ucla.edu**.

REFERENCES

1. B. B. Mandelbrot (1977). *Fractals: Form, Chance and Dimension*. Freeman, San Francisco.
2. R. Brooks & J. P. Matelski (1980). "The Dynamics of 2-Generator Subgroups of $PSL(2,C)$ ". In: *Riemann Surfaces and Related Topics: Proceedings of the 1978 Stony Brook Conference* (I. Kra & B. Maskit, eds.), Princeton University Press 1981.
3. B. B. Mandelbrot (1980). "Fractal Aspects of the Iteration of $z \rightarrow \lambda(1-z)$ for complex λ, z ." *Ann. N.Y. Acad. Sciences* **357**, 249–259.
4. A. Douady & J. H. Hubbard (1982). "Itération des Polynômes Quadratiques Complexes". *C. R. Acad. Sci. Paris Sér. I Math.* **294**, no. 3, 123–126.
5. B. B. Mandelbrot (1983). *The Fractal Geometry of Nature*. W. H. Freeman, New York.
6. H.-O. Peitgen & P. H. Richter (1986). *The Beauty of Fractals*. Springer-Verlag, Berlin.
7. H.-O. Peitgen & D. Saupe, Eds. (1988). *The Science of Fractal Images*. Springer-Verlag, Berlin
8. H.-O. Peitgen, H. Jürgens & D. Saupe (1992). *Chaos and Fractals: New Frontiers of Science*. Springer-Verlag, Berlin

